

Hypervalent Adducts of Chalcogen-Containing *peri*-Substituted Naphthalenes; Reactions of Sulfur, Selenium, and Tellurium with Dihalogens

Fergus R. Knight, Amy L. Fuller, Michael Bühl, Alexandra M. Z. Slawin, and J. Derek Woollins*

School of Chemistry, University of St. Andrews, St. Andrews, Fife, United Kingdom, KY16 9ST

Received May 29, 2010

A range of structurally diverse compounds **1–15** {Nap[SPh]₂·Br₄ (Nap = naphthalene-1,8-diyl); Nap[SePh][EPh]·Br₄ (E = Se, S); Nap[SePh]₂·I₂; Nap[SePh][EPh]·3/2I₂ (E = Se, S); Nap[TePh][G]·X₂ (G = SePh, SPh, Br, I; X = Br, I); and [Nap(PPh₂OH)(SPh)]⁺Br₃[−]} formed from the reactions between *peri*-substituted naphthalene chalcogen donors **D1–D8** {Nap[ER][E'R] (ER/E'R = SPh, SePh, TePh); Nap[TePh][X] (X = Br, I); and Nap[PPh₂][SPh]} and dibromine and diiodine were characterized by X-ray crystallography and where possible by multinuclear NMR, IR, and MS. X-ray data for **1–15** were analyzed by naphthalene ring torsions, *peri*-atom displacement, splay angle magnitude, *peri*-distance, aromatic ring orientations, and quasi-linear three-body arrangements. The hypervalent linear moieties are considered in the context of the charge-transfer model and the 3c–4e model introduced by Pimentel and Rundle. In general, the conformation of the final products obeyed the rule based on charge-transfer that “seesaw” (X–ER₂–X, 10-E-4) adducts arise when the halogen (X) is more electronegative than the chalcogen (E), and if the converse is true then, CT “spoke” (X–X–ER₂, 8-E-3) adducts are formed. Upon treatment with dibromine, selenium donor compounds **D2** {Nap[SePh]₂} and **D3** {Nap[SePh][SPh]} afford unusual tribromide salts of bromoselenyl cations containing a hypervalent X–E···E' 3c-4e type interaction. Upon treatment with diiodine, **D2** and **D3** form “Z-shaped”, “extended spoke” adducts containing an uncommon 2:3 donor/chalcogen ratio and incorporating chains of I₂ held together by rare I···I interactions. As expected, “seesaw” 10-E-4 adducts are formed following the reaction of Te donors **D4–D7** {Nap[TePh][X] (X = Br, I); Nap[TePh][EPh] (E = Se, S)} with the dihalogens. Naphthalene distortion in general is comparable between respective donor compounds and products **1–15**. Ionic species **2** and **3** display a noticeable reduction in molecular distortion explained by the relief of steric strain via weak *peri*-interactions and the onset of 3c–4e bonding.

1. Introduction

Hypervalency of the heavier main group elements has attracted considerable attention due to the extraordinary structures and reactivity their compounds exhibit. The ambiguity over the bonding in these species continues to intrigue chemists and has been debated upon since the pioneering work on the electronic theory of the covalent bond by Lewis and Langmuir in the early 1900s.^{1–4} While elements of period 2 and atoms in their lowest valences conformed readily to the octet rule, the bonding in molecules formed by heavier atoms of the periodic table in their higher valences (e.g., PCl₅) conflicted with this theory and was the topic of a contentious debate.^{2,4} Lewis persisted with his traditional theory of the

2c–2e covalent bond but proposed that the bonding was accompanied by an expansion of the octet.^{2,5} Conversely, Langmuir favored the octet rule and argued that the bonding was now ionic rather than covalent.^{2,6}

With the emergence of quantum mechanical theory, the bonding in hypervalent compounds was generally assumed to be covalent in nature and rationalized by the acceptance of the supplementary electrons into the unfilled low-lying d orbitals, thus violating the octet rule.^{3,4,7–9} The absence of 2d orbitals therefore justified the lack of hypervalency in compounds of period 2.^{3,4} With the advancement of molecular orbital theory, Rundle and Pimentel developed the earlier

(5) Lewis, G. N. In *Valence and the Structure of Atoms and Molecules*; The Chemical Catalog Co.: New York, 1923; chapter 8.

(6) Langmuir, I. *Science* **1921**, *54*, 59.

(7) (a) Hatch, R. J.; Rundle, R. E. *J. Am. Chem. Soc.* **1951**, *73*, 4321.

(b) Rundle, R. E. *J. Am. Chem. Soc.* **1963**, *85*, 112. (c) Rundle, R. E. *J. Am. Chem. Soc.* **1947**, *69*, 1327.

(8) (a) Mooney, R. C. L. *Z. Kristallogr.* **1935**, *90*, 143. (b) Mooney, R. C. L. *ibid* **1937**, *98*, 324.

(9) (a) Pauling, L. In *The Nature of the Chemical Bond*, 3rd ed.; Pauling, L., Ed.; Cornell University Press: Ithaca, NY, 1960; chapter 7. (b) Pauling, L. *J. Am. Chem. Soc.* **1947**, *69*, 542.

*To whom correspondence should be addressed. E-mail: jdw3@st-and.ac.uk.

(1) (a) Lewis, G. N. *J. Am. Chem. Soc.* **1916**, *38*, 762. (b) Langmuir, I. *J. Am. Chem. Soc.* **1919**, *41*, 868.

(2) Jensen, W. B. *J. Chem. Educ.* **2006**, *83*, 1751.

(3) Musher, J. I. *Angew. Chem., Int. Ed. Engl.* **1969**, *8*, 54.

(4) (a) *Inorganic Chemistry*; Shriver, D. F., Atkins, P. W., Eds.; Oxford University Press: Oxford, U. K., 1999; chapter 3, p 70. (b) *Basic Inorganic Chemistry*; Cotton, F. A., Wilkinson, G., Gaus, P. L., Eds.; John Wiley & Sons, Inc.: New York, 1995; p 74.

work undertaken by Sugden¹⁰ and introduced the notion of a three-center, four-electron bond (3c–4e) to explain the hypervalency in the trihalide ions.^{7,11} This concept has become a favored method for explaining the existence of hypervalency without violating the octet rule or invoking ionic bonding.^{12,13} The four electrons occupy bonding and nonbonding molecular orbitals;^{2,7,11,14,15} as only one bonding pair is available for the two bonds, hypervalent bonds are weaker than single electron pair bonds (2c–2e) between the same elements. Bond orders of apical bonds in hypervalent 3c–4e species are typically less than one (~0.5), with bond distances predicted to be 0.18 Å longer than for single electron pair bonds with bond orders of 1.0.^{7,9,11,14,15}

In 1969, Musher classified “hypervalent” molecules as those “formed by elements in Groups V–VIII of the periodic table in any of their valences other than their lowest stable chemical valence of 3, 2, 1, and 0 respectively.”³ The pertinence of the term “hypervalence” has recently been under dispute following the advancement of quantum mechanical calculations which reinforce the 3c–4e theory proposed by Rundle and Pimentel and conform to the octet rule.^{2,7,11,13,16} As a consequence, the use of octet expansion of the heavier main group elements has diminished from current bonding descriptions.^{13,16,17} Nonetheless, hypervalency is a topic of continued interest to chemists with numerous compounds containing linear arrangements of three main group elements having been well documented recently in the literature.^{14,15,18–22} The nature of the bonding in these linear species can be described by the Rundle–Pimentel 3c–4e model and a charge-transfer model and has recently been thoroughly reviewed.²³

Organic molecules containing the group 16 donor atoms sulfur, selenium, and tellurium react with dihalogens (Br₂, I₂) and interhalogens (IBr, ICl) to form a variety of addition complexes with wide structural diversity. Experimental conditions control the pathway these reactions take and subsequently the structural motifs and geometry around the group 16 atoms in the final structure. Factors such as the type of chalcogen donor atom, the form of the dihalogen or inter-

halogen, the stoichiometry of the reactants, and the nature of the donor atoms' R group(s) all play a significant role.^{15,22} A slight adjustment to any one of these variables could lead to subtle modifications in molecular geometry, so it is unsurprising that a diverse combination of structures have been synthesized: charge-transfer (CT) “spoke” and “extended spoke” adducts, polyiodide, “seesaw”, ionic, “T-shaped”, bent, mixed-valence, dication-bridged, and dimeric structural motifs.^{15,22} Ionic compounds, often accompanied by counteranions of polyhalides adopting unusual and sometimes complex structures are also known.^{15,22,24–33} The neutral charge-transfer (CT) “spoke” adduct (R₂E–X–Y, 8-E-3) and the “seesaw” (X–ER₂–Y, 10-E-4) insertion adduct, characteristic of quasi-linear hypervalent E–X–Y^{15,22,28,34,35} and X–E–Y^{14,15,22,28,31,36,37} fragments, respectively, are the most common structural motifs generated from the reaction of diorganochalcogen donors [R₂E] with inter- or dihalogens.

With variations in the reaction conditions affecting the outcome of reactions between chalcogen donors [R₂E] with di- and interhalogens, predicting the conformation of the final solid state structures continues to be a challenge to chemists. In solution, the CT “spoke” adduct and the “seesaw” adduct of RR'E·X₂ type compounds are in equilibrium.^{14,38,39} Husebye and co-workers suggested that all the products in these reactions are derived from a common intermediate species [R₂E–X]⁺ and progress via a general reaction pathway,^{15,22,40} with nucleophilic attack occurring

(10) Sugden, S. In *The Parachor and Valency*; Knopf: New York, 1930; chapter 6.

(11) Pimentel, G. C. *J. Chem. Phys.* **1951**, *19*, 446.

(12) (a) Coulson, C. A. d-Orbitals in Chemical Bonding. In *Proceedings of the Robert A. Welch Foundation Conferences on Chemical Research. XVI. Theoretical Chemistry*; Mulliken, W. O., Ed.; Houston, TX, 1972; chapter 3.

(b) Brill, T. B. *J. Chem. Educ.* **1973**, *50*, 392.

(13) (a) Kutzelnigg, W. *Angew. Chem., Int. Ed.* **1984**, *23*, 272. (b) *Valency and Bonding*; Weinhold, F., Landis, C., Eds.; Cambridge University Press: Cambridge, U.K., 2005; chapter 3.

(14) Nakanishi, W. In *Handbook of Chalcogen Chemistry, New Perspectives in Sulfur, Selenium and Tellurium*; Devillanova, F. A., Ed.; RSC Publishing: Cambridge, U. K., 2007; chapter 10.3 and references cited therein.

(15) Lippolis, V.; Isaia, F. In *Handbook of Chalcogen Chemistry*; Devillanova, F. A., Ed.; RSC Publishing: Cambridge, U. K., 2007; chapter 8.2 and references cited therein.

(16) Smith, D. W. *J. Chem. Educ.* **2005**, *82*, 1202.

(17) (a) Gillespie, R. J.; Robinson, E. A. *Inorg. Chem.* **1995**, *34*, 978.

(b) Noury, S.; Silvi, B.; Gillespie, R. J. *Inorg. Chem.* **2002**, *41*, 2164.

(18) *Chemistry of Hypervalent Compounds*; Akiba, K.-Y., Ed.; Wiley-VCH: New York, 1999.

(19) Landrum, G. A.; Goldberg, N.; Hoffmann, R. *J. Chem. Soc., Dalton Trans.* **1997**, 3605.

(20) Svensson, P. H.; Kloo, L. *Chem. Rev.* **2003**, *103*, 1649.

(21) Perkins, C. W.; Martin, J. C.; Arduengo, A. J.; Law, W.; Alegrie, A.; Kocki, J. K. *J. Am. Chem. Soc.* **1980**, *102*, 7753.

(22) Boyle, P. D.; Godfrey, S. M. *Coord. Chem. Rev.* **2001**, *223*, 265 and references cited therein.

(23) Aragoni, M. C.; Arca, M.; Demartin, F.; Devillanova, F. A.; Garau, A.; Isaia, F.; Lippolis, V.; Mancini, A. *Bioinorg. Chem. Appl.* **2007**, *2007*, 17416.

(24) Aragoni, M. C.; Arca, M.; Demartin, F.; Devillanova, F. A.; Garau, A.; Isaia, F.; Lippolis, V.; Verani, G. *J. Am. Chem. Soc.* **2002**, *124*, 4538.

(25) Aragoni, M. C.; Arca, M.; Devillanova, F. A.; Isaia, F.; Lippolis, V.; Mancini, A.; Pala, L.; Slawin, A. M. Z.; Woollins, J. D. *Chem. Commun.* **2003**, 2226.

(26) Demartin, F.; Deplano, P.; Devillanova, F. A.; Isaia, F.; Lippolis, V.; Verani, G. *Inorg. Chem.* **1993**, *32*, 3694.

(27) Bigoli, F.; Demartin, F.; Deplano, P.; Devillanova, F. A.; Isaia, F.; Lippolis, V.; Mercuri, M. L.; Pellinghelli, M. A.; Trogu, E. F. *Inorg. Chem.* **1996**, *35*, 3194.

(28) Aragoni, M. C.; Arca, M.; Demartin, F.; Devillanova, F. A.; Garau, A.; Isaia, F.; Lippolis, V.; Verani, G. *Trends Inorg. Chem.* **1999**, *6*, 1 and references cited therein.

(29) Boyle, P. D.; Christie, J.; Dyer, T.; Godfrey, S. M.; Howson, I. R.; McArthur, C.; Omar, B.; Pritchard, R. G.; Williams, G. Rh. *J. Chem. Soc., Dalton Trans.* **2000**, 3106.

(30) Daga, V.; Hadjikakou, S. K.; Hadjiliadis, N.; Kubicki, M.; dos Santos, J. H. Z.; Butler, I. S. *Eur. J. Inorg. Chem.* **2002**, 1718.

(31) Khun, N.; Fawzi, R.; Kratz, T.; Steimann, M.; Henkel, G. *Phosphorus, Sulfur Silicon Relat. Elem.* **1996**, *112*, 225.

(32) du Mont, W.-W. *Main Group Chem. News* **1994**, *2*, 18.

(33) Demartin, F.; Devillanova, F. A.; Isaia, F.; Lippolis, V.; Verani, G. *Inorg. Chim. Acta* **1997**, *255*, 203.

(34) Ouvrard, C.; Le Questel, J.-Y.; Berthelot, M.; Laurence, C. *Acta Crystallogr., Sect. B: Struct. Sci.* **2003**, *B59*, 512.

(35) Näther, C.; Bolte, M. *Phosphorus, Sulfur Silicon Relat. Elem.* **2003**, *178*, 453.

(36) Khun, N.; Kratz, T.; Henkel, G. *Z. Naturforsch. B, Chem. Sci.* **1996**, *51*, 295.

(37) Aragoni, M. C.; Arca, M.; Blake, A. J.; Devillanova, F. A.; du Mont, W.-W.; Garau, A.; Isaia, F.; Lippolis, V.; Verani, G.; Wilson, C. *Angew. Chem., Int. Ed. Engl.* **2001**, *40*, 4229.

(38) Nakanishi, W.; Hayashi, S.; Kihara, H. *J. Org. Chem.* **1999**, *64*, 2630.

(39) (a) Nakanishi, W.; Hayashi, S.; Tukada, H.; Iwamura, H. *J. Phys. Org. Chem.* **1990**, *3*, 358. (b) Nakanishi, W.; Yamamoto, Y.; Hayashi, S.; Tukada, H.; Iwamura, H. *J. Phys. Org. Chem.* **1990**, *3*, 369. (c) Nakanishi, W.; Hayashi, S. *J. Organomet. Chem.* **2000**, *611*, 178. (d) Nakanishi, W.; Hayashi, S. *Heteroat. Chem.* **2001**, *12*, 369. (e) Nakanishi, W.; Hayashi, S.; Kusuyama, Y. *J. Chem. Soc., Perkin Trans. 2* **2002**, 262. (f) Laur, P. H.; Saberi-Niaki, S. M.; Scheiter, M.; Hu, C.; Englert, U.; Wang, Y.; Fleischhauer, J. *Phosphorus, Sulfur Silicon Relat. Elem.* **2005**, *180*, 1035.

(40) Rudd, M. D.; Linderman, S. V.; Husebye, S. *Acta Chem. Scand.* **1997**, *51*, 689.

at the halogen and the chalcogen sites of the $[R_2E-X]^+$ cation affording the CT “spoke” and “seesaw” hypervalent adducts, respectively.^{14,15,22,41} The structure of the final product can therefore be predicted with a generalization based on the degree of charge transfer between the nonbonding orbitals of the chalcogen donor $n(E)$ to the LUMO of the di- or interhalogen acceptor $\sigma^*(X-X')$.^{14,39,42} This can be estimated from the electronegativity (χ) of the elements and follows the loose rule that the “seesaw” adducts will be formed if halide X is more electronegative than chalcogen E $[R_2E^{\delta+}-X^{\delta-}]$, while if the converse is true, then the CT “spoke” adducts will predominate.^{14,39,42} This is exemplified by the fact that no CT adducts are known for Te donors $[\chi(\text{Te}) 2.08]^{43}$ with any di- or interhalogen $[\chi(\text{F}) 3.94, \chi(\text{I}) 2.36]$.^{14,15,22,43} It must be recognized, however, that the electronegativity of the chalcogen atom and the electronic properties of R_2E can be affected by the R groups, thus influencing the outcome of the reaction. Compounds with bulky groups around E will favor the three-coordinate chalcogen environment of the CT “spoke” adduct over the more congested four-coordinate atom in the “seesaw” form.^{14,39}

“Spoke” adducts are formed via the transfer of electron density from nonbonding orbitals of the chalcogen donor atom into the LUMO of the di- or interhalogen acceptor molecule (and hence termed charge-transfer adducts). This generally occurs when $\chi(E) > \chi(X)$; i.e., the chalcogen atom is a stronger donor and more electron density is available to donate into the empty orbitals on X.^{15,22} The majority of neutral CT “spoke” adducts reported in the literature are formed by the reaction of organosulfur $[\chi(\text{S}) 2.58]^{43}$ donors with diiodine $[\chi(\text{I}) 2.36]$,^{15,22,30,35,43,44} for example, benzyl sulfide diiodine.⁴⁵

Organoselenium diiodine CT adducts are less common,^{15,22,46,47} but those reported in the literature exhibit a

considerable increase in the iodine–iodine bond length from free iodine $[2.66 \text{ \AA}]^{48}$ compared to similar sulfur compounds, showing that organoselenides are better donor molecules than organosulfides $[\chi(\text{Se}) 2.35, \chi(\text{S}) 2.58]$.^{15,22,43} Reaction of dibromine with diorganosulfur and diorganoselenium donors produces adducts of different geometries. Following the general rule based on electronegativity values, both R_2S $[\chi(\text{S}) 2.58]^{43}$ and $R_2\text{Se}$ $[\chi(\text{Se}) 2.35]^{43}$ donors are expected to form “seesaw” compounds $[\chi(X) > \chi(E); \chi(\text{Br}) 2.68]$.^{14,15,22,39,42,43} While all structurally reported diorganoselenium dibromine compounds exclusively adopt “seesaw” structures,^{14,15,22,47,49,50} diorganosulfur dibromine compounds are known to adopt CT “spoke” arrangements.^{15,22,28,42,51,52} (“T-shaped” adducts have been reported from the reaction of S-donor compounds with dibromine).^{41,53}

Generally, when the halide species (X) is more electronegative than the chalcogen atom (E), “T-shaped” or “seesaw” adducts are formed.^{14,39,42} Consequently, all the known reactions between tellurium donors $[\chi(\text{Te}) 2.08]^{43}$ and di- or interhalogens $[\chi(\text{F}) 3.94, \chi(\text{I}) 2.36]^{43}$ form “T-shaped” or “seesaw” adducts with no tellurium CT “spoke” adducts known.^{15,22,42} Tellurium forms strong donor–strong acceptor systems with the dihalogens, strong enough to cleave the X–X bond and oxidize tellurium.^{14,15,22} Subsequent nucleophilic attack occurring at the tellurium site of the $[R_2\text{Te}-X]^+$ cation affords the “seesaw”/“T-shaped” hypervalent adduct with a quasi linear X–Te–X alignment.^{14,15,22}

Partial negative charge acting on the terminal Y atom of the R_2E-X-Y linear fragment can be sufficient for CT “spoke” adducts to act as donors toward other acceptors (A). This produces adducts which are structurally more complex, known as CT “extended spoke” adducts $[R_2E-X-Y \cdots A]$ (where A is normally another XY molecule and $XY \cdots A$ angles are typically close to 90°).^{15,22} The terminal atom–acceptor ($Y \cdots A$) interaction delocalizes negative charge onto Y, which in turn strengthens the E–X bond. With an extremely strong $Y \cdots A$ interaction, systems of the type $[RE-X]^+[Y-A]^-$ can be envisaged (for example, the adduct formed by reaction of N-methylbenzothiazole-2(3H)-selenone with IBr).^{2,15}

- (41) (a) Aragoni, M. C.; Arca, M.; Demartin, F.; Devillanova, F. A.; Garau, A.; Isaia, F.; Lelj, F.; Lippolis, V.; Verani, G. *Chem.—Eur. J.* **2001**, *7*, 3122. (b) Aragoni, M. C.; Arca, M.; Demartin, F.; Devillanova, F. A.; Garau, A.; Isaia, F.; Lippolis, V.; Verani, G. *Dalton Trans.* **2005**, 2252.
- (42) Baenziger, M. C.; Buckles, R. E.; Maner, R. J.; Simpson, T. D. *J. Am. Chem. Soc.* **1969**, *91*, 5749.
- (43) (a) Allred, A. L.; Rochow, E. G. *J. Inorg. Nucl. Chem.* **1958**, *5*, 264. (b) Allred, A. L.; Rochow, E. G. *J. Inorg. Nucl. Chem.* **1958**, *5*, 269.
- (44) (a) Allen, D. W.; Berridge, R.; Bricklebank, N.; Forder, S. D.; Palacio, F.; Coles, S. J.; Hursthouse, M. B.; Skabara, P. J. *Inorg. Chem.* **2003**, *42*, 3975. (b) Bigoli, F.; Deplano, P.; Mercuri, M. L.; Pellinghelli, M. A.; Sabatini, A.; Trogu, E. F.; Vacca, A. *J. Chem. Soc., Dalton Trans.* **1996**, 3583. (c) Blake, A. J.; Devillanova, F. A.; Garau, A.; Gilby, L. M.; Gould, R. O.; Isaia, F.; Lippolis, V.; Parsons, S.; Radek, C.; Schröder, M. *J. Chem. Soc., Dalton Trans.* **1998**, 2037. (d) Arca, M.; Demartin, F.; Devillanova, F. A.; Garau, A.; Isaia, F.; Lippolis, V.; Verani, G. *J. Chem. Soc., Dalton Trans.* **1999**, 3069. (e) Hartl, H.; Steidl, S. *Z. Naturforsch. B, Chem. Sci.* **1977**, *32*, 6. (f) Lyon, E. J.; Musie, G.; Reibenspies, J. H.; Darensbourg, M. Y. *Inorg. Chem.* **1998**, *37*, 6942. (g) Ito, S.; Liang, H.; Yoshifuji, M. *Chem. Commun.* **2003**, 398. (h) Apperley, D. C.; Bricklebank, N.; Hursthouse, M. B.; Light, M. E.; Coles, S. J. *Polyhedron* **2001**, *20*, 1907. (i) Antoniadis, C. D.; Corban, G. J.; Hadjikakou, S. K.; Hadjiliadis, N.; Kubicki, M.; Warner, S.; Butler, I. S. *Eur. J. Inorg. Chem.* **2003**, 1635. (j) Cross, W. I.; Godfrey, S. M.; Jackson, S. L.; McAuliffe, C. A.; Pritchard, R. G. *J. Chem. Soc., Dalton Trans.* **1999**, 2225. (k) Corban, G. J.; Hadjikakou, S. K.; Hadjiliadis, N.; Kubicki, M.; Tiekink, E. R. T.; Butler, I. S.; Drougas, E.; Kosmas, A. M. *Inorg. Chem.* **2005**, *44*, 8617.
- (45) Romming, C. *Acta Chem. Scand.* **1960**, *14*, 2145.
- (46) (a) Chao, G. Y.; McCullough, J. D. *Acta Crystallogr.* **1961**, *14*, 940. (b) Hope, H.; McCullough, J. D. *Acta Crystallogr.* **1962**, *15*, 806. (c) Hope, H.; McCullough, J. D. *Acta Crystallogr.* **1964**, *17*, 712. (d) Maddox, H.; McCullough, J. D. *Inorg. Chem.* **1966**, *5*, 522. (e) Jeske, J.; du Mont, W.-W.; Jones, P. G. *Chem.—Eur. J.* **1999**, *5*, 385. (f) Cristiani, F.; Demartin, F.; Devillanova, F. A.; Isaia, F.; Saba, G.; Verani, G. *J. Chem. Soc., Dalton Trans.* **1992**, 3553.
- (47) Godfrey, S. M.; McAuliffe, C. A.; Pritchard, R. G.; Sarwar, S. *J. Chem. Soc., Dalton Trans.* **1997**, 1031.

(48) *Chemistry of the Elements*; Greenwood, N. N., Earnshaw, A., Eds.; Reed Elsevier: Oxford, U. K., 1997.

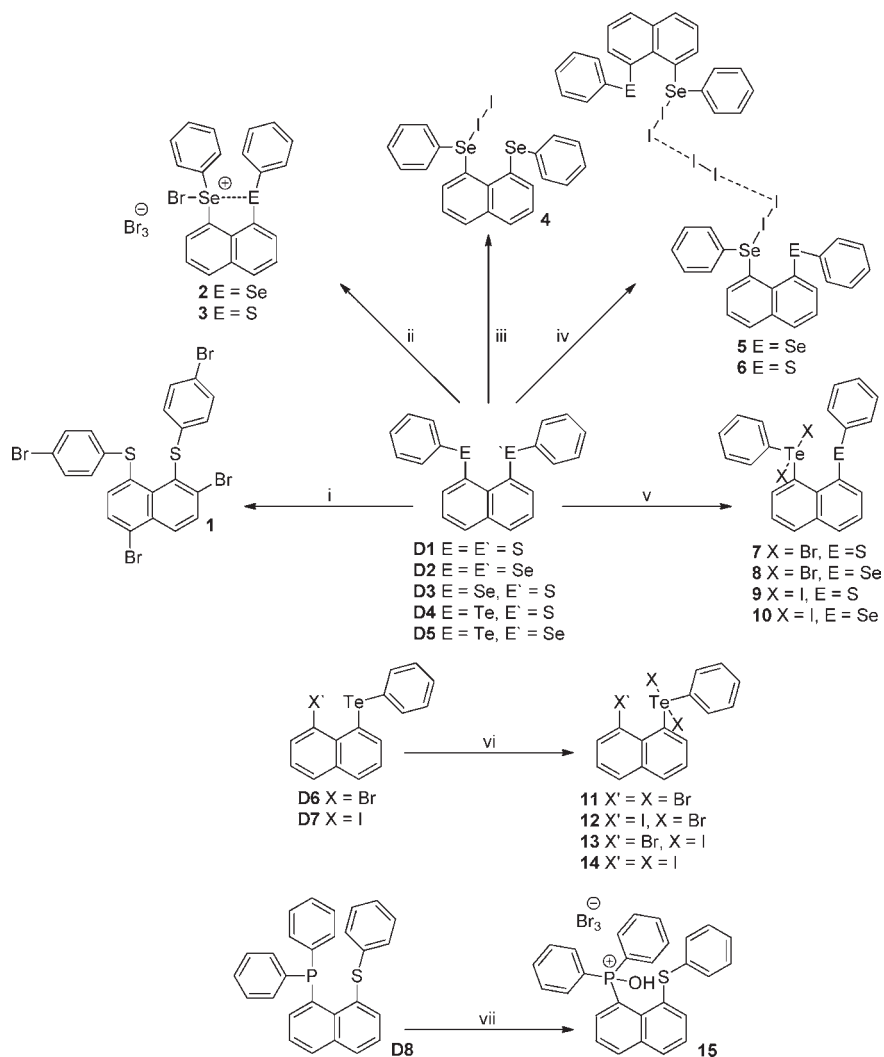
(49) (a) McCullough, J. D.; Marsh, R. E. *Acta Crystallogr.* **1950**, *3*, 41. (b) Barlow, M.; Zimmermann-Barlow, I. *Acta Chem. Scand. (Moscow Abstr.)* **1966**, *21*, A103. (c) Battelle, L.; Knobler, C.; McCullough, J. D. *Inorg. Chem.* **1967**, *6*, 958.

(50) McCullough, J. D.; Hamburger, G. *J. Am. Chem. Soc.* **1941**, *63*, 803. (51) (a) Allegra, G.; Wilson, G. E., Jr.; Benedetti, E.; Pedone, C.; Albert, R. *J. Am. Chem. Soc.* **1970**, *92*, 4002. (b) Haywood, G. C.; Hendra, P. J. *J. Chem. Soc. A* **1969**, 1760. (c) Regelman, B.; Klinkhammer, K. W.; Schmidt, A. Z. *Anorg. Allg. Chem.* **1997**, *623*, 1633. (d) Vaughan, G. B. M.; Mora, A. J.; Fitch, A. N.; Gates, P. N.; Muir, A. S. *J. Chem. Soc., Dalton Trans.* **1999**, 79.

(52) Vaughan, G. B. M.; Mora, A. J.; Fitch, A. N.; Gates, P. N.; Muir, A. S. *J. Chem. Soc., Dalton Trans.* **1999**, 79.

(53) (a) Regelman, B.; Klinkhammer, K. W.; Schmid, A. Z. *Anorg. Allg. Chem.* **1988**, *562*, 42. (b) Bricklebank, N.; Skabara, P. J.; Hibbs, D. E.; Hursthouse, M. B.; Malik, K. M. A. *J. Chem. Soc., Dalton Trans.* **1999**, 3007.

(54) (a) Aucott, S. M.; Milton, H. L.; Robertson, S. D.; Slawin, A. M. Z.; Walker, G. D.; Woollins, J. D. *Chem.—Eur. J.* **2004**, *10*, 1666. (b) Aucott, S. M.; Milton, H. L.; Robertson, S. D.; Slawin, A. M. Z.; Woollins, J. D. *Heteroat. Chem.* **2004**, *15*, 530. (c) Aucott, S. M.; Milton, H. L.; Robertson, S. D.; Slawin, A. M. Z.; Woollins, J. D. *Dalton Trans.* **2004**, 3347. (d) Aucott, S. M.; Kilian, P.; Milton, H. L.; Robertson, S. D.; Slawin, A. M. Z.; Woollins, J. D. *Inorg. Chem.* **2005**, *44*, 2710. (e) Aucott, S. M.; Kilian, P.; Robertson, S. D.; Slawin, A. M. Z.; Woollins, J. D. *Chem.—Eur. J.* **2006**, *12*, 895. (f) Aucott, S. M.; Duerden, D.; Li, Y.; Slawin, A. M. Z.; Woollins, J. D. *Chem.—Eur. J.* **2006**, *12*, 5495.

Scheme 1. Hypervalent Adducts Formed from the Reactions of Chalcogen-Containing *peri*-Substituted Naphthalenes **D1–D8** with Dibromine and Diiodine^a

^a conditions: (i–vii) X₂ (X = Br, I), CH₂Cl₂, 2 h, RT; i (4 equiv), Br₂; ii (2 equiv), X₂; iii/iv (1 equiv), I₂; v/vi (1 equiv), X₂; vii (4 equiv), Br₂.

We have previously explored sterically crowded 1,8-disubstituted naphthalenes.^{54,55} Our early work focused on dichalcogenide ligands⁵⁴ and unusual phosphorus compounds.⁵⁵ More recently, we have reported the synthesis and structural study of mixed phosphorus–chalcogen,⁵⁶ chalcogen–chalcogen,⁵⁷ and halogen–chalcogen systems.⁵⁸ During our investigations of *peri*-substituted naphthalenes, we prepared

a number of chalcogen donors **D1–D8** (Scheme 1).^{57,58} The work reported here complements our previous study of chalcogen–naphthalene derivatives,^{56–58} expanding the knowledge of naphthalene distortion and contributing to the exciting field of hypervalence that occurs in linear species formed from the reactions between chalcogen donors and dihalogens. Here, we present the reactions between chalcogen donors **D1–D8** and dibromine and diiodine and a full structural study of the geometrically diverse products formed, **1–15** (Scheme 1).

2. Results and Discussion

Compounds **1–15** were synthesized, and where possible the derivatives were characterized by multinuclear NMR and IR spectroscopy and mass spectrometry. The homogeneity of the new compounds was confirmed by microanalysis.³¹P, ⁷⁷Se, and ¹²⁵Te NMR spectroscopy data for compounds **4–15** are compared in Table 1 with those of donors **D2–D8**.^{57,58} The tribromide salts **2** and **3** are insoluble in all common NMR solvents; hence, no NMR spectroscopic data for these compounds are given. Suitable single crystals were obtained for **1–15** by diffusion of pentane into

(55) (a) Kilian, P.; Philp, D.; Slawin, A. M. Z.; Woollins, J. D. *Eur. J. Inorg. Chem.* **2003**, 249. (b) Kilian, P.; Slawin, A. M. Z.; Woollins, J. D. *Chem.—Eur. J.* **2003**, 9, 215. (c) Kilian, P.; Slawin, A. M. Z.; Woollins, J. D. *Chem. Commun.* **2003**, 1174. (d) Kilian, P.; Slawin, A. M. Z.; Woollins, J. D. *Dalton Trans.* **2003**, 3876. (e) Kilian, P.; Milton, H. L.; Slawin, A. M. Z.; Woollins, J. D. *Inorg. Chem.* **2004**, 43, 2252. (f) Kilian, P.; Slawin, A. M. Z.; Woollins, J. D. *Inorg. Chim. Acta* **2005**, 358, 1719. (g) Kilian, P.; Slawin, A. M. Z.; Woollins, J. D. *Dalton Trans.* **2006**, 2175.

(56) (a) Knight, F. R.; Fuller, A. L.; Slawin, A. M. Z.; Woollins, J. D. *Dalton Trans.* **2009**, 8476. (b) Knight, F. R.; Fuller, A. L.; Slawin, A. M. Z.; Woollins, J. D. *Chem.—Eur. J.* **2010**, 16, 7617. (c) Knight, F. R.; Fuller, A. L.; Slawin, A. M. Z.; Woollins, J. D. *Polyhedron*, **2010**, 29, 1849, DOI: 10.1016/j.poly.2010.02.033. (d) Knight, F. R.; Fuller, A. L.; Slawin, A. M. Z.; Woollins, J. D. *Polyhedron*, **2010**, 29, 1956, DOI: 10.1016/j.poly.2010.03.006.

(57) Knight, F. R.; Fuller, A. L.; Bühl, M.; Slawin, A. M. Z.; Woollins, J. D. *Chem.—Eur. J.* **2010**, 16, 7503.

(58) Knight, F. R.; Fuller, A. L.; Bühl, M.; Slawin, A. M. Z.; Woollins, J. D. *Chem.—Eur. J.* **2010**, 16, 7605.

saturated solutions of the individual compound in dichloromethane. All compounds **1–15** crystallize with one molecule in the asymmetric unit. Selected interatomic distances, angles, and torsion angles are listed in Tables 1–6. Further crystallographic information can be found in Tables 8–11 and the Supporting Information.

Table 1. ^{31}P , ^{77}Se , and ^{125}Te NMR Spectroscopy Data [δ (ppm)] for Donors **D2–D8** and Adducts **4–15**

	D2	4	5	D3	6	
peri atoms	SeSe	SeSe	SeSe	SeS	SeS	
X–Te–X		Se–I–I	Se–I–I···I ₂		Se–I–I···I ₂	
^{77}Se NMR	428.6	436.9, 436.7	445.1, 444.3	455.3	476.9	
	D4	7	9	D5	8	10
peri atoms	TeS	TeS	TeS	TeSe	TeSe	TeSe
X–Te–X		Br–Te–Br	I–Te–I		Br–Te–Br	I–Te–I
^{77}Se NMR				362.8	500.0	428.8
^{125}Te NMR	715.2	958.9	790.9	687.6	941.4	747.0
	D6	11	13	D7	12	14
peri atoms	BrTe	BrTe	BrTe	ITe	ITe	ITe
X–Te–X		Br–Te–Br	I–Te–I		Br–Te–Br	I–Te–I
^{125}Te NMR	731.2	942.8	887.5	698.3	903.0	848.0
	D8			15		
peri-atoms	PS			PS		
^{31}P NMR	–5.3			52.5		

Table 2. Selected Interatomic Distances [\AA] and Angles [deg] for **1–5**

compound	1	2	3	4	5
peri-region distances and subvan der Waals contacts					
E(1)···E'(1)	2.935(4)	2.7619(7)	2.721(2)	3.1339(6)	3.0756(14)
$\Sigma r_{\text{vdw}} - E \cdots E'$; % Σr_{vdw}^a	0.665; 82	1.038; 73	0.979; 74	0.666; 82	0.724; 81
E(1)–C(1)	1.787(11)	1.957(6)	1.955(8)	1.953(5)	1.948(8)
E'(1)–C(9)	1.780(11)	1.918(5)	1.796(9)	1.933(5)	1.929(7)
naphthalene bond lengths					
C(1)–C(2)	1.365(16)	1.372(8)	1.375(14)	1.366(7)	1.375(15)
C(2)–C(3)	1.388(16)	1.401(9)	1.390(15)	1.411(8)	1.410(12)
C(3)–C(4)	1.370(16)	1.352(9)	1.342(17)	1.383(8)	1.350(17)
C(4)–C(5)	1.417(15)	1.424(8)	1.424(14)	1.374(8)	1.428(16)
C(5)–C(10)	1.453(15)	1.430(8)	1.429(12)	1.451(7)	1.430(11)
C(5)–C(6)	1.438(16)	1.404(8)	1.422(16)	1.416(8)	1.406(14)
C(6)–C(7)	1.340(18)	1.357(9)	1.363(16)	1.350(8)	1.365(17)
C(7)–C(8)	1.386(16)	1.395(9)	1.404(15)	1.393(8)	1.411(13)
C(8)–C(9)	1.402(16)	1.374(8)	1.362(15)	1.379(7)	1.376(14)
C(9)–C(10)	1.431(15)	1.414(7)	1.395(13)	1.424(7)	1.412(14)
C(10)–C(1)	1.442(15)	1.427(7)	1.450(14)	1.435(6)	1.441(14)
peri-region bond angles					
E(1)–C(1)–C(10)	122.3(8)	119.8(4)	119.5(6)	121.9(3)	122.5(7)
C(1)–C(10)–C(9)	126.0(10)	126.2(5)	126.0(8)	128.4(4)	126.9(7)
E'(1)–C(9)–C(10)	121.6(8)	120.1(4)	119.8(7)	123.0(4)	124.2(6)
Σ of bay angles	369.9(18)	366.1(9)	365.3(15)	373.3(7)	373.6(14)
splay angle ^b	9.9	6.1	5.3	13.3	13.6
C(4)–C(5)–C(6)	121.0(10)	120.6(5)	119.0(8)	119.9(5)	119.2(8)
out-of-plane displacement					
E(1)	–0.343(13)	0.2887(66)	0.112(11)	–0.3290(74)	0.415(11)
E'(1)	0.343(13)	–0.0101(66)	0.139(11)	0.5359(73)	–0.246(11)
central naphthalene ring torsion angles					
C:(6)–(5)–(10)–(1)	176.1(10)	–177.4(12)	179.3(8)	–172.7(7)	176.7(6)
C:(4)–(5)–(10)–(9)	176.2(9)	–175.0(12)	–179.2(8)	–176.2(7)	174.8(7)

^a van der Waals radii used for calculations: $r_{\text{vdw}}(\text{S})$, 1.80 \AA ; $r_{\text{vdw}}(\text{Se})$, 1.90 \AA ; ^b Splay angle: Σ of the three bay region angles – 360.

Adducts formed from the reaction of diorganosulfur compounds with dibromine are rare. The majority of those reported and structurally characterized by single-crystal X-ray diffraction adopt the CT “spoke” structure with a S–Br–Br linear arrangement.^{15,22,28,42,51} Upon treatment of 1,8-bis(phenylsulfanyl)naphthalene **D1** with dibromine, no adduct is isolated, but electrophilic aromatic substitution dominates. Aromatic groups bearing –SR groups are strongly activated by delocalization of resonance lone pairs into the aromatic π system and are therefore highly reactive toward electrophilic substitution.⁵⁹ The delocalization of the lone pair on sulfur into the aromatic system in **D1** makes it unavailable for donation into the empty orbitals of the dibromine molecule. The naphthalene ring system being less aromatic than the phenyl moieties thus makes it more susceptible toward electrophilic substitution. The activating S(phenyl) group donates electrons into the π system and directs incoming electrophiles to the *ortho* or *para* positions. Attack at the *para* position is sterically more favorable, placing the large bromine atom further from the bulk of the molecule.⁵⁹ The second bromination is directed by the second S(phenyl) moiety to the *ortho* (C7) position to avoid the inevitable steric interaction between the bromine atoms upon *para* substitution. Final bromination of the phenyl rings occurs with the sulfur atoms directing the substitution to the two *para* positions, away from the steric bulk of the molecule to produce 1,8-bis(4-bromophenylsulfanyl)-2,5-dibromonaphthalene **1**

Table 3. Selected Interatomic Distances [Å] and Angles [deg] for 6–10

compound	6	7	8	9	10
peri-region distances and subvan der Waals contacts					
E(1)···E'(1)	2.9798(18)	3.075(2)	3.141(2)	3.0767(17)	3.137(2)
$\Sigma r_{vdW} - E \cdots E'$; % Σr_{vdW}^a	0.720; 81	0.785; 80	0.819; 79	0.783; 78	0.823; 79
E(1)–C(1)	1.958(5)	2.124(10)	2.148(15)	2.138(6)	2.14(2)
E'(1)–C(9)	1.773(5)	1.782(11)	1.933(14)	1.784(6)	1.915(19)
naphthalene bond lengths					
C(1)–C(2)	1.367(9)	1.355(15)	1.36(2)	1.380(9)	1.43(2)
C(2)–C(3)	1.411(8)	1.410(16)	1.37(2)	1.395(10)	1.42(2)
C(3)–C(4)	1.360(11)	1.393(15)	1.39(2)	1.363(10)	1.37(3)
C(4)–C(5)	1.416(10)	1.400(15)	1.39(2)	1.411(10)	1.43(3)
C(5)–C(10)	1.427(7)	1.421(14)	1.45(2)	1.433(9)	1.41(3)
C(5)–C(6)	1.432(10)	1.452(15)	1.52(2)	1.420(9)	1.45(2)
C(6)–C(7)	1.361(11)	1.343(15)	1.28(2)	1.360(10)	1.36(2)
C(7)–C(8)	1.399(9)	1.388(15)	1.40(2)	1.405(10)	1.43(2)
C(8)–C(9)	1.360(10)	1.362(15)	1.34(2)	1.382(9)	1.36(3)
C(9)–C(10)	1.424(9)	1.447(14)	1.43(2)	1.447(9)	1.46(3)
C(10)–C(1)	1.431(9)	1.427(13)	1.42(2)	1.433(9)	1.43(2)
peri-region bond angles					
E(1)–C(1)–C(10)	121.7(4)	123.1(7)	122.2(10)	122.5(4)	122.6(14)
C(1)–C(10)–C(9)	126.8(5)	127.6(9)	130.4(15)	127.1(6)	129.4(17)
E'(1)–C(9)–C(10)	122.4(4)	121.3(7)	120.9(13)	122.7(5)	120.4(14)
Σ of bay angles	370.9(9)	372.0(16)	373.5(27)	372.3(11)	372.4(31)
splay angle ^b	10.9	12.0	13.5	12.3	12.4
C(4)–C(5)–C(6)	119.1(5)	117.7(9)	119.2(14)	119.4(6)	116.2(18)
out-of-plane displacement					
E(1)	0.438(11)	–0.401(12)	–0.444(1)	–0.3690(82)	–0.372(8)
E'(1)	–0.233(11)	0.250(12)	0.259(1)	0.3007(77)	0.317(8)
central naphthalene ring torsion angles					
C:(6)–(5)–(10)–(1)	176.8(4)	–179.1(8)	–177.0(12)	–177.3(6)	179.7(14)
C:(4)–(5)–(10)–(9)	174.9(4)	–174.3(8)	–173.5(13)	–174.1(5)	–174.7(13)

^a van der Waals radii used for calculations: $r_{vdW}(S)$, 1.80 Å; $r_{vdW}(Se)$, 1.90 Å; $r_{vdW}(Te)$, 2.06 Å. ^b Splay angle: Σ of the three bay region angles – 360.

(Scheme 1).⁵⁹ Varying the loading of dibromine (1–6 equiv) produced **1** exclusively.

Substitution of the heavier main group elements at the *peri* positions in naphthalene causes considerable steric hindrance, giving rise to structurally distorted compounds with unusual bonding and geometry.^{56–58,60} The bulky atoms are constrained in close proximity to the rigid backbone at a distance shorter than the sum of van der Waals radii for the two interacting atoms.^{56–58} Steric strain caused by the crowding of substituents can be released through bond formation or if weak attractive noncovalent interactions exist between tightly packed atoms.^{60,61} As nonbonded distances decrease relative to the sum of van der Waals radii, weak noncovalent interactions become more covalent in nature and the steric interaction

is reduced.⁶² Distortion away from the “ideal” naphthalene geometry also helps alleviate steric strain and occurs via in-plane and out-of-plane deviations of the exocyclic bonds and buckling of the usually rigid backbone.^{56–58,60,61,63} X-ray structural data play a fundamental role in determining naphthalene distortion and therefore assessing steric strain.^{56–58}

The structural geometry of compounds **1–15** can be described by the orientation of the naphthyl and phenyl rings relative to the C(ar)–G(1)–C(ar) and the C(ar)–Z(2)–CI planes, calculated from torsion angles θ and γ , respectively (see Table 7, Figure 1).⁶⁴ When θ and γ approach 90°, the orientation is categorized as axial, while an equatorial conformation is denoted by angles close to 180°. ⁶⁴ Conformations in between axial and equatorial are classified as twist.⁶⁴ For angle θ , axial conformations correspond to the “type A” structure presented by Nakanishi et al. (the G–C_{Ph}/Z–C_{Ph} bond lies perpendicular to the naphthyl plane).⁶⁵

(62) Hayashi, S.; Nakanishi, W. *Bull. Chem. Soc. Jpn.* **2008**, *81*(12), 1605.

(63) (a) Coulson, C. A.; Daudel, R.; Robertson, J. M. *Proc. R. Soc. London, Ser. A* **1951**, *A207*, 306. (b) Cruickshank, D. W. J. *Acta Crystallogr.* **1957**, *10*, 504. (c) Brock, C. P.; Dunitz, J. D. *Acta Crystallogr., Sect. B: Struct. Sci.* **1982**, *B38*, 2218. (d) Oddershede, J.; Larsen, S. J. *Phys. Chem. A* **2004**, *108*, 1057.

(64) Nagy, P.; Szabó, D.; Kapovits, I.; Kucsman, Á.; Argay, G.; Kálmán, A. *J. Mol. Struct.* **2002**, *606*, 61.

(65) (a) Nakanishi, W.; Hayashi, S. *J. Org. Chem.* **2002**, *67*, 38. (b) Hayashi, S.; Yamane, K.; Nakanishi, W. *J. Org. Chem.* **2007**, *72*, 7587. (c) Nakanishi, W.; Hayashi, S.; Toyota, S. *J. Am. Chem. Soc.* **1998**, *63*, 8790. (d) Nakanishi, W.; Hayashi, S.; Uehara, T. *J. Phys. Chem.* **1999**, *103*, 9906. (e) Nakanishi, W.; Hayashi, S.; Uehara, T. *Eur. J. Org. Chem.* **2001**, 3933.

(59) (a) *Organic Chemistry*; Clayden, J.; Greeves, N.; Warren, S.; Wothers, P., Eds.; Oxford University Press: Oxford, U. K., 2001; chapter 22. (b) *Organic Chemistry Structure and Function*, 3rd ed.; Vollhardt, K. P. C., Schore, N. E., Eds.; W. H. Freeman and Company: New York, 1999; chapter 16.

(60) Balasubramanian, V. *Chem. Rev.* **1966**, *66*, 567.

(61) (a) Schmidbaur, H.; Öller, H.-J.; Wilkinson, D. L.; Huber, B.; Müller, G. *Chem. Ber.* **1989**, *122*, 31. (b) Fujihara, H.; Furukawa, N. *J. Mol. Struct.* **1989**, *186*, 261. (c) Fujihara, H.; Akaishi, R.; Erata, T.; Furukawa, N. *J. Chem. Soc., Chem. Commun.* **1989**, 1789. (d) Handal, J.; White, J. G.; Franck, R. W.; Yuh, Y. H.; Allinger, N. L. *J. Am. Chem. Soc.* **1977**, *99*, 3345. (e) Blount, J. F.; Cozzi, F.; Damewood, J. R.; Iroff, D. L.; Sjöstrand, U.; Mislow, K. *J. Am. Chem. Soc.* **1980**, *102*, 99. (f) Anet, F. A. L.; Donovan, D.; Sjöstrand, U.; Cozzi, F.; Mislow, K. *J. Am. Chem. Soc.* **1980**, *102*, 1748. (g) Hounshell, W. D.; Anet, F. A. L.; Cozzi, F.; Damewood, J. R., Jr.; Johnson, C. A.; Sjöstrand, U.; Mislow, K. *J. Am. Chem. Soc.* **1980**, *102*, 5941. (h) Schröck, R.; Angermaier, K.; Sladek, A.; Schmidbaur, H. *Organometallics* **1994**, *13*, 3399.

Table 4. Selected Interatomic Distances [Å] and Angles [deg] for **11–15**

compound	11	12	13	14	15
peri-region distances and sub van der Waals contacts					
G(1)···E(1)	3.2397(15)	3.3810(7)	3.1563(6)	3.3608(11)	3.165(2)
$\Sigma r_{vdw} - G \cdots E$; % Σr_{vdw}^a	0.670; 83	0.659; 84	0.754; 81	0.679; 83	0.435; 88
G(1)–C(1)	1.900(11)	2.117(9)	1.911(6)	2.097(11)	1.796(11)
E(1)–C(9)	2.153(10)	2.150(8)	2.150(6)	2.159(9)	1.789(12)
naphthalene bond lengths					
C(1)–C(2)	1.382(16)	1.361(13)	1.357(9)	1.384(17)	1.393(13)
C(2)–C(3)	1.413(16)	1.397(14)	1.390(10)	1.369(17)	1.391(17)
C(3)–C(4)	1.341(18)	1.376(14)	1.360(8)	1.36(2)	1.359(13)
C(4)–C(5)	1.423(17)	1.422(13)	1.409(10)	1.392(16)	1.423(14)
C(5)–C(10)	1.450(14)	1.453(12)	1.424(8)	1.432(13)	1.442(17)
C(5)–C(6)	1.427(18)	1.410(14)	1.419(7)	1.423(16)	1.415(13)
C(6)–C(7)	1.357(16)	1.352(14)	1.364(9)	1.345(16)	1.362(14)
C(7)–C(8)	1.390(15)	1.416(13)	1.405(8)	1.400(15)	1.414(18)
C(8)–C(9)	1.345(17)	1.374(14)	1.362(6)	1.354(16)	1.397(13)
C(9)–C(10)	1.441(16)	1.437(13)	1.444(8)	1.450(14)	1.420(12)
C(10)–C(1)	1.415(16)	1.406(13)	1.421(6)	1.415(17)	1.459(12)
peri-region bond angles					
G(1)–C(1)–C(10)	121.3(8)	122.0(6)	121.5(4)	126.3(7)	126.2(7)
C(1)–C(10)–C(9)	129.3(10)	129.3(8)	128.1(5)	128.2(8)	126.4(10)
E(1)–C(9)–C(10)	122.5(8)	124.6(6)	122.8(3)	124.2(7)	122.9(7)
Σ of bay angles	373.1(18)	375.9(14)	372.4(9)	378.7(15)	375.5(17)
splay angle ^b	13.1	15.9	12.4	18.7	15.5
C(4)–C(5)–C(6)	119.9(9)	119.8(8)	119.4(5)	120.5(10)	118.9(11)
out-of-plane displacement					
G(1)	–0.550(14)	–0.644(14)	0.312(14)	–0.410(14)	0.436(11)
E(1)	0.641(15)	0.646(15)	–0.614(14)	0.436(14)	–0.466(11)
central naphthalene ring torsion angles					
C(6)–(5)–(10)–(1)	170.2(10)	–168.7(8)	174.4(5)	–175.2(9)	171.9(7)
C(4)–(5)–(10)–(9)	174.0(10)	–175.5(8)	176.5(5)	–176.8(9)	174.9(7)

^a van der Waals radii used for calculations: $r_{vdw}(P)$, 1.80 Å; $r_{vdw}(S)$, 1.80 Å; $r_{vdw}(Br)$, 1.85 Å; $r_{vdw}(I)$, 1.98 Å; $r_{vdw}(Te)$, 2.06 Å.^{61 b} Splay angle: Σ of the three bay region angles – 360.

Table 5. Selected Interatomic X–E–E, E–X–X, and X₃[–] distances [Å] and angles [deg] for **2–6**

compound	2	3	4	5	6
E–Se–X and Br ₃ [–] distances and subvan der Waals contacts			Se–I–I and I ₃ [–] distances and subvan der Waals contacts		
Br(1)–Se(1)	2.4878(8)	2.4232(15)	I(1)–Se(1)	2.9795(8)	2.8497(9)
Se(1)–E(2)	2.7619(8)	2.721(2)	I(1)–I(2)	2.7987(6)	2.8672(8)
Br(2)–Br(3)	2.5170(8)	2.5514(17)	I(2)···I(3)		3.543(1)
Br(3)–Br(4)	2.5668(8)	2.5433(17)	I(3)–I(3) ¹		2.7402(11)
			I(1)···E(2)	3.6956(7)	3.8730(9)
					2.7418(7)
					3.8527(13)
E–E–X and E–X–X bond angles					
Br(1)–Se(1)–E(2)	172.10(3)	176.34(1)	I(2)–I(1)–Se(1)	177.637(15)	178.09(3)
Br(2)–Br(3)–Br(4)	177.78(3)	178.57(5)	I(2)···I(3)–I(3) ¹		177.5(1)
			I(1)–I(2)···I(3)		176.3(1)
			I(1)–Se(1)–E(2)	74.33(1)	81.54(1)
					82.81(1)

An equatorial conformation for θ aligns the G–C_{Ph}/Z–C_{Ph} bond on or close to the plane (“type B”),⁶⁵ and a twist conformation relates to Nakanishi’s “type C” (Figure 1).^{64,65}

Compound **1** (Figure 2) displays a mixed equatorial–axial and axial–equatorial conformation of naphthyl and phenyl rings around the two individual sulfur atoms, matching that observed for **D1** and classified as the “AB-type” structure (Figure 1).^{57,65} The sulfur atoms are displaced to even distances but to opposite sides of the naphthalene least-squares plane with a deviation comparable to that displayed by **D1**.⁵⁷ The sulfur atoms are further accommodated by in-plane

distortions in the C–C–C group between the *peri* atoms indicated by a positive splay angle of 9.9°. The resulting nonbonded S···S *peri* distance [2.935(4) Å] is 18% shorter than the sum of the van der Waals radii for two sulfur atoms [3.60 Å]⁶⁶ and marginally shorter than that observed in **D1** [3.0036(13) Å].⁵⁷

A more pronounced distortion of the naphthalene skeleton is observed in **1**, which exhibits larger maximum C–C–C–C torsion angles [*ca.* 4°] compared to **D1** [*ca.* 1–3°].⁵⁷ Br(4) and

(66) Bondi, A. *J. Phys. Chem.* **1964**, *68*, 441.

Br(8) atoms lie 0.025(13) Å and 0.103(11) Å above the naphthyl plane, respectively, and Br–C [1.90–1.91 Å] and S–C [1.79–1.76 Å] bond lengths are within the usual ranges [1.90, 1.77 ± 0.05 Å]. Intermolecular short contacts exist between bromine atoms [Br(4)···Br(8)¹ 3.63(1) Å; Br(4)···Br(14)¹¹ 3.65(1) Å; Br(14)···Br(20)¹¹ 3.63(1) Å], but no significant overlap of phenyl or naphthyl rings is observed.

All structurally reported adducts formed from the reaction of diorganoselenium compounds with dibromine adopt the “seesaw” geometry.^{14,15,22,47,49,50} The donor compounds 1,8-bis(phenylselenyl)naphthalene **D2** and 1-(phenylselenyl)-8-(phenylsulfanyl)naphthalene **D3** react with dibromine to form similar tribromide salts of analogous bromoselenyl cations, which can be represented by the formula [RSe–Br]⁺···[Br–Br]₂[–] (Scheme 1).¹⁵ The lower electronegativity and hence greater electron donor ability of selenium over sulfur allows for a strong donor–strong acceptor system to form with dibromine sufficient to cleave the Br–Br bond and oxidize the selenium atom.^{15,22,43} In both **D2** and **D3**, the Se(1) atom reacts with the first molecule of Br₂ simultaneously weakening the Br(1)–Br(2) bond. The partial negative charge acting on the terminal Br(2) atom could be sufficient to act as a donor toward a second (acceptor) molecule of Br₂. Delocalization of negative charge onto the terminal Br(2) atom would strengthen the Se(1)–Br(1) bond

to the extent that the Br(1)–Br(2) bond is cleaved, forming the cation [RSe–Br]⁺ and a quasi-linear hypervalent 3c–4e Br₃[–] counteranion.¹⁵

The ionic “extended spoke” adducts **2** and **3** adopt a similar conformation in their molecular structures (Figure 3). The naphthyl and phenyl rings orient with an axial–equatorial arrangement around each chalcogen *peri* atom with both E–C_{Ph} bonds aligning perpendicular to and on the same side of the naphthyl plane (“AA-*c* type”, Figure 1).^{64,65} The phenyl rings overlap in a face-to-face offset arrangement with centroid–centroid distances [**2**, 3.691(1) Å; **3**, 3.79(1) Å] within the usual range for typical π–π stacking [3.3–3.8 Å].⁶⁷ Each adduct displays one quasi-linear X–E···E' arrangement of three atoms [**2**, 172.1°; **3**, 176.3°], the nature of the bonding that can be described by the Rundle–Pimentel 3c–4e model.^{7,11} The Se···Se and Se···S *peri* distances in **2** and **3** [2.7619(7) Å; 2.721(2) Å] are 27% and 26% shorter than the sum of van der Waals radii for the two interacting atoms, respectively. These values lie between those of a single electron pair Se–Se and Se–S bond [2.3639(5) Å; 2.24(1) Å]^{68,69} and the nonbonding interactions observed in **D2** and **D3** [3.1332(9) Å; 3.063(2) Å], respectively.⁵⁷

The significant reduction in the *peri* distance in both adducts relative to **D2** and **D3** suggests that a weak attractive noncovalent interaction is operating between the *peri* atoms, thus decreasing steric hindrance. As expected, naphthalene distortion in **2** and **3**, although still influential due to the absence of a strong *peri*-covalent bond,⁶⁸ is notably diminished compared with **D2** and **D3**, respectively. The inclination of the exocyclic E–C_{Nap} bonds within the naphthyl plane is minimal with small, but not negligible, positive splay angles [**2**, 6.1°; **3**, 5.3°] considerably reduced compared with donor compounds **D2** [13.9°] and **D3** [12.4°]. The displacement of the *peri* atoms from the naphthyl plane is relatively low in both compounds, with the Se(2) atom of **2** lying virtually on the plane. The *peri* atoms of **3** are displaced to the same side of the plane. The naphthalene skeleton for **2** shows a minor deviation from planarity with central naphthalene ring torsion angles *ca.* 3–5°, while the backbone of **3** is essentially planar *ca.* 0.7–0.8°.

Table 6. Selected Interatomic X–E–X Distances [Å] and Angles [deg] for **7–14**

compound	7	8	9	10
X–E–X distances, sub van der Waals contacts, and bond angles				
X(1)–Te(1)	2.7072(11)	2.719(2)	2.9457(6)	2.9538(17)
Te(1)–X(2)	2.6688(12)	2.671(2)	2.9073(6)	2.8943(17)
X(1)···G(1) ^a	3.486(2)	3.542(2)	3.6136(16)	3.696(2)
X(1)–Te(1)–X(2)	176.67(4)	177.94(6)	176.81(2)	179.59(6)
	11	12	13	14
X(1)–Te(1)	2.6664(13)	2.6578(10)	2.9343(5)	2.9480(7)
Te(1)–X(2)	2.6686(13)	2.6779(11)	2.8952(4)	2.9042(7)
X(1)···G(1) ^a	3.7079(17)	3.8497(11)	4.0089(6)	4.16(1)
X(1)–Te(1)–X(2)	175.80(4)	176.55(3)	176.405(19)	177.27(3)

^aG(1) = S, **7, 9**; Se, **8, 10**; Br, **11, 13**; I, **12, 14**.

Table 7. Torsion Angles [deg] Categorizing the Naphthalene and Phenyl Ring Conformations in **1–15**^a

	naphthalene ring conformations		phenyl ring conformations	
	Nap ₁ : C(10)–C(1)–G(1)–C(11)	Nap ₂ : C(10)–C(9)–Z(9)–C(17)	Ph ₁ : C(1)–G(1)–C(11)–C(12)	Ph ₂ : C(9)–Z(9)–C(17)–C(18)
1	θ ₁ = 155.1(9): eq	θ ₂ = –105.3(9): ax	γ ₁ = –88.5(11): ax	γ ₂ = 16.8(12): eq
2	θ ₁ = 99.8(4): ax	θ ₂ = –101.4(4): ax	γ ₁ = 167.7(4): eq	γ ₂ = 164.4(4): eq
3	θ ₁ = 87.7(7): ax	θ ₂ = –116.3(7): ax	γ ₁ = –159.4(7): eq	γ ₂ = –151.5(8): eq
4	θ ₁ = –155.6(5): eq	θ ₂ = –88.9(5): ax	γ ₁ = –116.5(5): ax	γ ₂ = 170.2(4): eq
5	θ ₁ = 166.1(5): eq	θ ₂ = 75.1(6): ax	γ ₁ = –67.7(7): ax	γ ₂ = 26.2(9): eq
6	θ ₁ = 166.8(3): eq	θ ₂ = 75.2(4): ax	γ ₁ = 117.0(4): ax	γ ₂ = 23.2(7): eq
7	θ ₁ = –145.9(7): twist	θ ₂ = 85.8(8): ax	γ ₁ = –148.9(8): twist	γ ₂ = 148.3(8): twist
8	θ ₁ = –147.1(12): twist	θ ₂ = –86.4(13): ax	γ ₁ = 40.5(14): twist	γ ₂ = –29.5(16): twist
9	θ ₁ = –146.9(5): twist	θ ₂ = –87.5(5): ax	γ ₁ = –151.2(5): twist	γ ₂ = 146.2(5): twist
10	θ ₁ = –148.0(12): twist	θ ₂ = –86.8(13): ax	γ ₁ = 42.8(15): twist	γ ₂ = –21.8(17): twist
11	θ ₁ = 141.8(8): twist	n/a	γ ₁ = 137.0(8): twist	n/a
12	θ ₁ = –140.3(8): twist	n/a	γ ₁ = –136.5(7): twist	n/a
13	θ ₁ = 152.8(4): eq	n/a	γ ₁ = 138.6(4): twist	n/a
14	θ ₁ = –157.3(7): eq	n/a	γ ₁ = –135.7(8): twist	n/a
15	θ ₁ = 160.4(7) Nap ₁ : eq θ ₃ = –84.7(8) Nap ₃ : ax	θ ₂ = 97.8(6) Nap ₂ : ax	γ ₁ = 101.8(10) Ph ₁ : ax γ ₃ = 153.6(6) Ph ₃ : twist	γ ₂ = –168.1(7) Ph ₂ : eq

^aNap₁: naphthalene ring G(1). Nap₂: naphthalene ring Z(9). Nap₃: second naphthalene ring G(1). Ph₁: G(1) phenyl ring. Ph₂: Z(9) phenyl ring. Ph₃: second G(1) phenyl ring. ax = axial: perpendicular to C(ar)–G/Z–C(ar) plane. eq = equatorial: coplanar with C(ar)–G/Z–C(ar) plane. twist: intermediate between equatorial and axial.

Table 8. Crystallographic Data for Compounds 1–4

compound	1	2	3	4
empirical formula	C ₂₂ H ₁₂ Br ₄ S ₂	C ₁₆ H ₁₁ Br ₄ Se ₂	C ₂₂ H ₁₆ Br ₄ SSe	C ₂₂ H ₁₆ I ₂ Se ₂
fw	660.07	757.9	711	692.1
temperature (°C)	−148(1)	−148(1)	−148(1)	−148(1)
cryst color, habit	yellow, prism	orange, block	orange, platelet	orange, prism
cryst dimensions (mm ³)	0.12 × 0.06 × 0.06	0.12 × 0.12 × 0.12	0.18 × 0.12 × 0.06	0.12 × 0.12 × 0.06
cryst syst	monoclinic	monoclinic	monoclinic	triclinic
lattice params	<i>a</i> = 32.535(13) Å <i>b</i> = 5.4833(18) Å <i>c</i> = 27.215(9) Å β = 92.729(11)°	<i>a</i> = 9.293(3) Å <i>b</i> = 14.082(5) Å <i>c</i> = 17.212(6) Å β = 97.177(9)°	<i>a</i> = 13.555(2) Å <i>b</i> = 9.2381(13) Å <i>c</i> = 18.663(3) Å β = 103.009(3)°	<i>a</i> = 10.003(3) Å <i>b</i> = 10.453(2) Å <i>c</i> = 11.749(3) Å α = 102.307(6)° β = 84.68(3)° γ = 93.395(4)° <i>V</i> = 1089.3(5)
volume (Å ³)	<i>V</i> = 4850(3)	<i>V</i> = 2234.8(13)	<i>V</i> = 2277.0(6)	<i>V</i> = 1089.3(5)
space group	<i>C</i> 2/ <i>c</i>	<i>P</i> 2 ₁ / <i>n</i>	<i>P</i> 2 ₁ / <i>c</i>	<i>P</i> $\bar{1}$
<i>Z</i> value	8	4	4	2
Dcalc (g/cm ³)	1.808	2.252	2.074	2.11
F000	2528	1424	1352	644
μ(Mo Kα) (cm ^{−1})	68.368	104.897	87.882	62.337
no. of reflns measd	13347	13998	12771	11727
Rint	0.068	0.042	0.064	0.036
min and max transmissions	0.406–0.664	0.268–0.284	0.294–0.590	0.486–0.688
independent reflns	4268	4524	3971	3715
obsd refln (no. variables)	3398(254)	3974(254)	3489(254)	3557(236)
refln/param ratio	16.8	17.81	15.63	15.74
residuals: <i>R</i> ₁ (<i>I</i> > 2.00σ(<i>I</i>))	0.0866	0.0435	0.0699	0.0302
residuals: <i>r</i> (all reflns)	0.1144	0.054	0.0813	0.0359
residuals: <i>wR</i> ₂ (all reflns)	0.2732	0.1236	0.1938	0.1262
goodness of fit indicator	1.206	1.175	1.15	1.28
Flack param				
maximum peak in final diff. map	2.78 e/Å ³	1.32 e/Å ³	2.33 e/Å ³	1.44 e/Å ³
minimum peak in final diff. map	−1.00 e/Å ³	−1.17 e/Å ³	−1.18 e/Å ³	−1.77 e/Å ³

The linear Br₃[−] counteranions present in both molecular structures exhibit a lengthening of the Br–Br distances [2.52–2.57 Å] compared to free bromine [2.28 Å].⁴⁸ This is indicative of the three-center, four-electron bond (3c–4e) model proposed by Rundle and Pimentel to explain hypervalency in the trihalide ions.^{7,11} The primary distinction between the molecular structures of **2** and **3** derives from differing intra- and intermolecular interactions and subsequent molecular packing. Short Br(1)⋯Br(2) [3.172(1) Å] and Se(2)¹⋯Br(2) [3.555(1) Å] contacts present in **2** lock two neighboring molecules together, forming a quasi-planar rectangular arrangement of eight atoms (Figure 4). Two further nonbonded intermolecular interactions are observed between a terminal Br(4¹¹) atom of a Br₃[−] ion and the two selenium peri atoms [Se(1)⋯Br(4¹¹) 3.250(1) Å and Se(2)⋯Br(4¹¹) 3.715(1) Å]. The linear tribromide counteranion in **3** adopts a position above the *peri* atoms. There is no Br(1)⋯Br₃[−] interaction but instead a nonbonded intramolecular interaction between Se(1)⋯Br(2) [3.562(1) Å]. Although a number of short contacts exist, there is no significant overlap of phenyl or naphthyl rings in either adduct and no π⋯π stacking.

Diorganoselenium compounds are known to form CT “spoke” adducts upon treatment with diiodine.^{15,22,46,47} 1,8-Bis(phenylselenyl)naphthalene **D2** reacts with one molar equivalent of diiodine to form the neutral CT “spoke” adduct **4** containing a quasi-linear Se–I–I fragment [177.6(1)°]

(Scheme 1). Iodine [χ(I) 2.36],⁴³ unlike bromine [χ(Br) 2.68],⁴³ has a similar electronegativity to selenium [χ(Se) 2.35]⁴³ and accepts electron density from nonbonding orbitals of the selenium donor to form the charge-transfer adduct. This has the effect of lowering the bond order and consequently weakening the I–I bond, which extends from 2.66 Å (free iodine)⁴⁸ to 2.7987(6) Å.^{15,22} The partial negative charge delocalized on the terminal I(2) atom in the hypervalent 3c–4e Se(1)–I(1)–I(2) bond allows I(2) to act as a donor toward a second molecule of diiodine to afford a CT “extended spoke” adduct **5** (Scheme 1).¹⁵

Adduct **5** adopts a similar structure to that formed by the reaction of triphenylphosphine sulfide with I₂.⁷⁰ The terminal iodine atoms of two molecules of adduct **4** (D2–I₂) act as donors toward the same diiodine molecule, which bridges via soft–soft I⋯I interactions [3.543(1) Å], constructing a “Z-shaped” system with a **D2**–I₂⋯I₂⋯**D2** configuration. Compounds with extended poly(I₂) chains held by weak I₂⋯I₂ interactions and adducts formed with a donor/dihalogen composition greater than 1:1 are extremely rare.^{15,71}

The treatment of 1-(phenylselenyl)-8-(phenylsulfanyl)naphthalene **D3** with two equivalents of diiodine produces an analogous “Z-shaped” adduct to that of **5** (Scheme 1). Two “spoke”-like adduct units constructed from the selenium donor moiety of **D3** and diiodine are bridged by the same diiodine molecule with weak I⋯I interactions of a similar magnitude as observed in adduct **5** [3.526(1) Å].¹⁵

The ⁷⁷Se NMR spectra for adducts **4** and **5** display a downfield shift compared to **D2** [δ = 428.6 ppm].⁵⁷ Both spectra exhibit two signals, each corresponding to a different

(67) (a) Roesky, H. W.; Andruh, M. *Coord. Chem. Rev.* **2003**, *236*, 91.(b) Koizumi, T.; Tsutsui, K.; Tanaka, K. *Eur. J. Org. Chem.* **2003**, 9(18), 4528.(c) Janiak, C. *J. Chem. Soc., Dalton Trans.* **2000**, 3885.(68) Fuller, A. L.; Knight, F. R.; Slawin, A. M. Z.; Woollins, J. D. *Eur. J. Inorg. Chem.* **2010**, accepted.(69) Meinwald, J.; Dauplaise, D.; Clardy, J. *J. Am. Chem. Soc.* **1977**, *99* (23), 7743.(70) (a) Schweikert, W. W.; Meyers, E. A. *J. Phys. Chem.* **1968**, *72*, 1561.(b) Bransford, J. W.; Meyers, E. A. *Cryst. Struct. Commun.* **1978**, *7*, 697.(71) Arca, M.; Demartin, F.; Devillanova, F. A.; Garau, A.; Isaia, F.; Lippolis, V.; Verani, G. *J. Chem. Soc., Dalton Trans.* **1999**, 3069.

Table 9. Crystallographic Data for Compounds 5–8

compound	5	6	7	8
empirical formula	C ₄₄ H ₃₂ I ₆ Se ₄	C ₄₄ H ₃₂ I ₆ Se ₂ Se ₂	C ₂₂ H ₁₆ Br ₂ STe	C ₂₂ H ₁₆ Br ₂ SeTe
fw	1638	1544.2	599.84	646.73
temperature (°C)	−148(1)	−148(1)	−148(1)	−180(1)
cryst color, habit	red, prism	red, prism	yellow, prism	colorless, platelet
cryst dimensions (mm ³)	0.15 × 0.09 × 0.09	0.21 × 0.15 × 0.09	0.21 × 0.03 × 0.03	0.06 × 0.06 × 0.03
cryst syst	triclinic	triclinic	monoclinic	monoclinic
lattice params	<i>a</i> = 9.6503(18) Å <i>b</i> = 11.3357(16) Å <i>c</i> = 11.8269(16) Å α = 65.996(10)° β = 82.763(14)° γ = 83.206(14)°	<i>a</i> = 9.6066(17) Å <i>b</i> = 11.2528(14) Å <i>c</i> = 11.8080(14) Å α = 65.855(9)° β = 82.839(14)° γ = 83.443(14)°	<i>a</i> = 18.873(10) Å <i>b</i> = 15.452(7) Å <i>c</i> = 13.922(6) Å β = 100.423(11)°	<i>a</i> = 19.172(8) Å <i>b</i> = 15.285(6) Å <i>c</i> = 14.070(7) Å β = 100.442(13)°
volume (Å ³)	<i>V</i> = 1169.3(3)	<i>V</i> = 1152.9(3)	<i>V</i> = 3993(3)	<i>V</i> = 4055(3)
space group	P $\bar{1}$	P $\bar{1}$	C2/c	C2/c
Z value	1	1	8	8
Dcalc (g/cm ³)	2.326	2.224	1.995	2.119
F000	750	714	2288	2432
μ(Mo Kα) (cm ^{−1})	71.303	57.432	56.13	7.207
no. of reflns measd	13845	13510	10797	12736
Rint	0.043	0.038	0.082	0.1295
min and max transmissions	0.336–0.526	0.403–0.596	0.542–0.845	0.652–1.000
independent reflns	4628	4542	3510	3669
obsd refln (no. variables)	4222(245)	4336(245)	2992(236)	2284(236)
refln/param ratio	18.89	18.54	14.87	15.55
residuals: <i>R</i> ₁ (<i>I</i> > 2.00σ(<i>I</i>))	0.0483	0.0429	0.0696	0.0947
residuals: <i>r</i> (All reflns)	0.0569	0.0479	0.0876	0.1436
residuals: <i>wR</i> ₂ (all reflns)	0.1746	0.1587	0.1808	0.2625
goodness of fit indicator	1.185	1.148	1.261	1.077
Flack param				
maximum peak in final diff. map	1.32 e/Å ³	2.46 e/Å ³	1.50 e/Å ³	2.515 e/Å ³
minimum peak in final diff. map	−1.56 e/Å ³	−1.98 e/Å ³	−1.67 e/Å ³	−1.557 e/Å ³

Table 10. Crystallographic Data for Compounds 9–12

compound	9	10	11	12
empirical formula	C ₂₂ H ₁₆ I ₂ STe	C ₂₂ H ₁₆ I ₂ SeTe	C ₁₆ H ₁₁ Br ₃ Te	C ₁₆ H ₁₁ Br ₂ ITe
fw	693.84	740.71	570.57	617.58
temperature (°C)	−148(1)	−180(1)	−148(1)	−148(1)
cryst color, habit	orange, prism	colorless, platelet	colorless, platelet	yellow, prism
cryst dimensions (mm ³)	0.15 × 0.09 × 0.09	0.05 × 0.05 × 0.05	0.12 × 0.12 × 0.01	0.15 × 0.09 × 0.09
cryst syst	monoclinic	monoclinic	orthorhombic	orthorhombic
lattice params	<i>a</i> = 18.909(4) Å <i>b</i> = 15.954(3) Å <i>c</i> = 14.282(3) Å β = 99.994(5)° <i>V</i> = 4243.1(15)	<i>a</i> = 19.723(9) Å <i>b</i> = 15.191(6) Å <i>c</i> = 14.463(6) Å β = 100.692(12)° <i>V</i> = 4258(3)	<i>a</i> = 8.4839(18) Å <i>b</i> = 12.041(2) Å <i>c</i> = 15.592(3) Å <i>V</i> = 1592.8(6)	<i>a</i> = 8.5238(18) Å <i>b</i> = 12.165(3) Å <i>c</i> = 15.780(3) Å <i>V</i> = 1636.3(6)
volume (Å ³)				
space group	<i>P</i> 2/c	<i>C</i> 2/c	<i>P</i> ca2 ₁	<i>P</i> ca2 ₁
Z value	8	8	4	4
Dcalc (g/cm ³)	2.172	2.311	2.379	2.507
F000	2576	2720	1056	1128
μ(Mo Kα) (cm ^{−1})	44.16	6.011	94.028	85.916
no. of reflns measd	12261	13494	4898	4932
Rint	0.033	0.1378	0.057	0.04
min and max transmissions	0.487–0.672	0.797–1.000	0.409–0.910	0.290–0.462
independent reflns	4204	3836	2459	2609
obsd refln (no. variables)	3961(236)	2117(236)	2353(182)	2579(182)
refln/param ratio	17.81	16.25	13.51	14.34
residuals: <i>R</i> ₁ (<i>I</i> > 2.00σ(<i>I</i>))	0.0361	0.0823	0.0461	0.0313
residuals: <i>r</i> (all reflns)	0.0429	0.1495	0.0503	0.0332
residuals: <i>wR</i> ₂ (all reflns)	0.1341	0.2132	0.0996	0.0967
goodness of fit indicator	1.244	0.992	1.089	1.206
Flack param				
maximum peak in final diff. map	1.65 e/Å ³	3.359 e/Å ³	0.77 e/Å ³	1.41 e/Å ³
minimum peak in final diff. map	−1.63 e/Å ³	−1.375 e/Å ³	−1.09 e/Å ³	−1.50 e/Å ³

selenium environment [**4**, δ = 436.9, 436.7 ppm; **5**, δ = 445.1, 444.3 ppm]. The ⁷⁷Se NMR spectrum for adduct **6** reveals a similar downfield shift compared to **D3** [δ = 455.3 ppm]⁵⁷ with a single peak at δ = 476.9 ppm.

Following the treatment of selenium donor **D2** with diiodine, no significant alteration to the naphthalene geo-

metry is observed upon the formation of the CT “spoke” addition product **4** (Figure 5).⁵⁷ The naphthyl and phenyl rings orient with the same mixed equatorial–axial/axial–equatorial conformation as observed for **D2**, with one E–C_{Ph} bond aligning perpendicular to the naphthyl plane and one aligning with the plane (“AB-type”, Figure 1).^{57,64,65}

Table 11. Crystallographic Data for Compounds 13–15

compound	13	14	15
empirical formula	C ₁₆ H ₁₁ BrI ₂ Te	C ₁₆ H ₁₁ I ₃ Te	C ₅₆ H ₄₃ O ₂ P ₂ S ₂ Br ₃
fw	664.58	711.58	1113.73
temperature (°C)	−148(1)	−148(1)	−148(1)
cryst color, habit	red, platelet	orange, prism	colorless, prism
cryst dimensions (mm ³)	0.15 × 0.15 × 0.03	0.12 × 0.03 × 0.03	0.12 × 0.09 × 0.09
cryst syst	triclinic	triclinic	triclinic
lattice params	<i>a</i> = 8.221(2) Å <i>b</i> = 9.639(3) Å <i>c</i> = 11.613(3) Å α = 105.274(8)° β = 90.454(4)° γ = 102.945(9)° <i>V</i> = 863.0(4)	<i>a</i> = 7.290(4) Å <i>b</i> = 9.642(6) Å <i>c</i> = 13.294(7) Å α = 104.034(9)° β = 92.232(12)° γ = 103.475(12)° <i>V</i> = 877.0(9)	<i>a</i> = 9.1606(13) Å <i>b</i> = 11.537(3) Å <i>c</i> = 12.606(4) Å α = 83.21(5)° β = 71.33(4)° γ = 66.89(4)° <i>V</i> = 1160.8(7)
volume (Å ³)			
space group	<i>P</i> $\bar{1}$	<i>P</i> $\bar{1}$	<i>P</i> $\bar{1}$
Z value	2	2	1
Dcalc (g/cm ³)	2.557	2.695	1.593
F000	600	636	562
μ (Mo K α) (cm ^{−1})	76.13	69.675	28.176
no. of reflns measd	9862	9605	11962
Rint	0.044	0.071	0.105
min and max transmissions	0.335 - 0.796	0.632 - 0.811	0.511 - 0.776
independent reflns	3384	3429	4041
obsd refln (no. variables)	3262(182)	3196(182)	3185(296)
refln/param ratio	18.59	18.84	13.65
residuals: <i>R</i> ₁ (<i>I</i> > 2.00 σ (<i>I</i>))	0.0373	0.0589	0.1109
residuals: <i>r</i> (All reflns)	0.0391	0.0675	0.1398
residuals: <i>wR</i> ₂ (all reflns)	0.1186	0.1966	0.1854
goodness of fit indicator	1.144	1.134	1.241
Flack param			
maximum peak in final diff. map	1.43 e/Å ³	2.28 e/Å ³	0.93 e/Å ³
minimum peak in final diff. map	−1.29 e/Å ³	−2.40 e/Å ³	−0.79 e/Å ³

Displacement of the *peri* atoms from the naphthalene mean plane in **4** is comparable to **D2** [*ca.* 0.3–0.5 Å]⁵⁷ and reveals that steric strain operating between the selenium atoms in the two compounds is of a similar magnitude. Deviation of the *peri* atoms within the naphthyl plane also corresponds, with the divergence of the exocyclic bonds illustrated by the splay angle [**4**, 13.3°; **D2**, 13.9°].⁵⁷ Despite the amount of naphthalene distortion, interatomic nonbonded Se···Se separations for **4** [3.1339(6)] and **D2** [3.1332(9)]⁵⁷ are 18% shorter than double the van der Waals radii of selenium [3.80].⁶⁶ Maximum C–C–C central naphthalene ring torsion angles in the range 4–7° show that both naphthalene backbones are significantly buckled.

The hypervalent quasi-linear Se(1)–I(1)–I(2) fragment [Se–I–I angle, 177.6°], characteristic of the weaker 3c–4e bond, displays an increase in the I(1)–I(2) bond length [2.7987(6) Å] compared to free diiodine [2.66 Å].⁴⁸ It is situated at 97.0(1)° to the Se(1)–C(11) bond and lies quasi-perpendicular to the C(11)–Se(1)–C(1) plane [76.6(1)°] due to steric crowding around the selenium lone pairs.^{72,73} This results in a close intramolecular I(1)···Se(2) contact [3.6956(7) Å], which is within the sum of van der Waals radii for interacting selenium and iodine atoms [3.88 Å].⁶⁶ Adduct **4** also exhibits an intermolecular nonbonded interaction between the I(2) and Se(2) atoms of neighboring molecules (A and B) with an I(2A)···Se(2B) distance of 3.663(1) Å (Figure 6).

The CT “extended spoke” adducts **5** and **6** are characterized by a “Z-shaped” D–I₂···I₂···D system constructed from two “spoke”-like adduct units and a bridging

diiodine molecule held by weak I···I interactions [5 3.543(1) Å; 6 3.526(1) Å] (Figure 7). In both cases, the linear Se–I–I fragment [**5**, 178.1(1)°; **6**, 179.0(1)°] has the same orientation as described for adduct **4**: situated at 99.4(1)° and 99.3(1)° to the Se(1)–C(11) bond and lying 80.4(1)° and 76.9(1)° from the C(11)–Se(1)–C(1) plane, respectively. I(1) is positioned in the *peri* gap with I(1)···E(2) separations [**5**, 3.8730(9) Å; **6**, 3.8527(13) Å] within the sum of van der Waals radii.⁶⁶

The interaction between the terminal I(2) atom of the “spoke” adduct and the second I₂ molecule weakens and extends the I(1)–I(2) bond [**5**, 2.8672(8) Å; **6**, 2.8706(5) (cf. **4**, 2.7987(6) Å)], concurrent with shortening the Se(1)–I(1) bond [**5**, 2.8497(9) Å; **6**, 2.8436(6) Å (cf. **4**, 2.9795(8) Å)].^{15,22} I(1)–I(2)···I₂ angles [**5**, 107.9(1)°; **6**, 108.0(1)°] are slightly more obtuse than average values [90°] for known “extended spoke” compounds.^{15,22} As expected, the I(3)–I(3¹) bond length of the bridging diiodine molecule is extended in both adducts [**5**, 2.7402(11) Å; **6**, 2.7418(7) Å] compared with free iodine [2.66 Å]⁴⁸ due to the existence of the weak I···I interactions.

The naphthalene components of each “Z-shaped” adduct display a minor decrease in molecular distortion compared with donor compounds **D2** and **D3**, with a greater distortion observed in adduct **5** compared with **6**. In both compounds, the nonbonded Se(1)···E(2) distance [**5**, 3.0756(14) Å; **6**, 2.9798(18) Å] is 19% shorter than the sum of van der Waals radii for the two interacting atoms [cf. **D2**, 18%; **D3**, 17%].⁵⁷ The displacement of the *peri* atoms from the naphthalene mean plane [0.2–0.4 Å] is comparable in the two adducts to the out-of-plane distortion observed for **D2** and **D3**.⁵⁷ The substitution of heavier elements in the bay region of **5** compared with **6** causes a larger positive splay of the two E–C_{Nap} bonds within the least-squares plane and thus exhibits a greater splay angle [**5**, 13.6°; **6**, 10.9°]. Maximum

(72) Ouvrard, C.; Le Questel, J.-Y.; Berthelot, M.; Laurence, C. *Acta Crystallogr., Sect. B: Struct. Sci.* **2003**, *59*, 512.

(73) Näther, C.; Bolte, M. *Phosphorus, Sulfur Silicon Relat. Elem.* **2003**, *178*, 453.

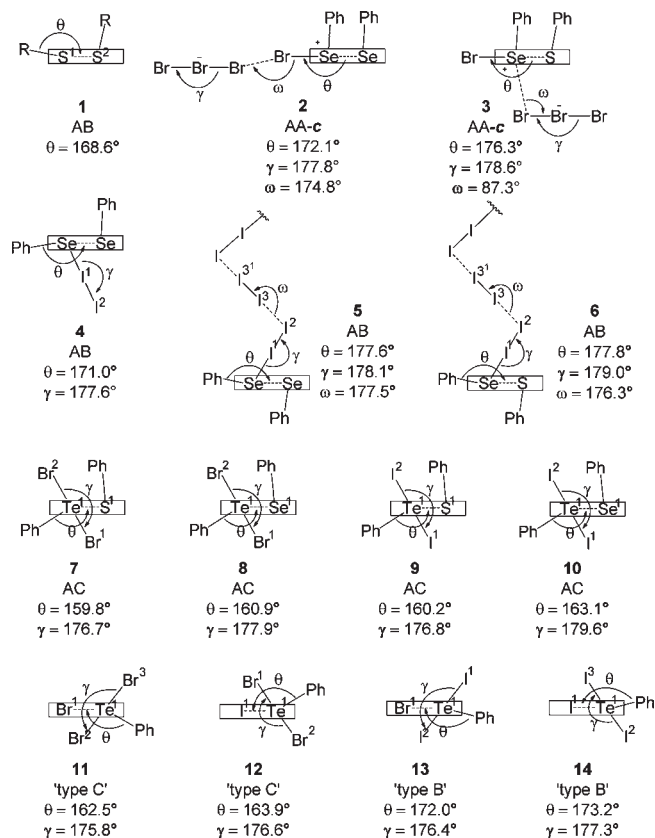


Figure 1. Orientation of the naphthyl and phenyl rings, the type of structure, and the quasi-linear arrangements in compounds 1–14.⁶⁵

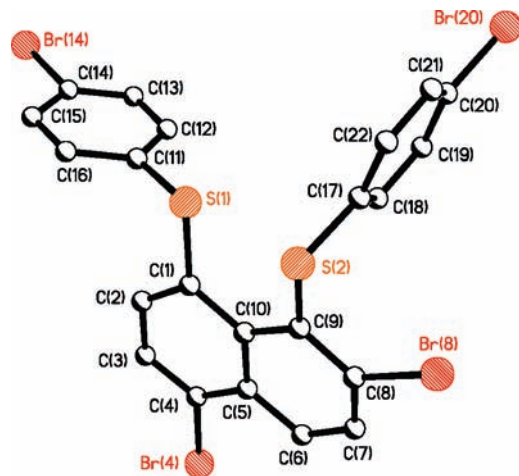


Figure 2. Molecular structure of 1,8-bis(4-bromophenylsulfanyl)-2,5-dibromonaphthalene 1.

C–C–C–C central ring torsion angles are in the range 3–5° for both compounds, showing that the deviation of the naphthalene backbones from planarity is comparable. The conformation of the naphthyl and phenyl rings in both adducts is comparable to donor compounds **D2** and **D3**, with an equatorial–axial/axial–equatorial orientation described as an “AB-type” structure.^{57,64,65}

“Seesaw” and “T-shaped” adducts are formed if halide X is more electronegative than chalcogen E [$R_2E^{\delta+}-X^{\delta-}$]. Consequently, all known reactions between tellurium donors [$\chi(\text{Te}) 2.08$]⁴³ and di- or interhalogens [$\chi(\text{F}) 3.94$, $\chi(\text{I}) 2.36$]⁴³

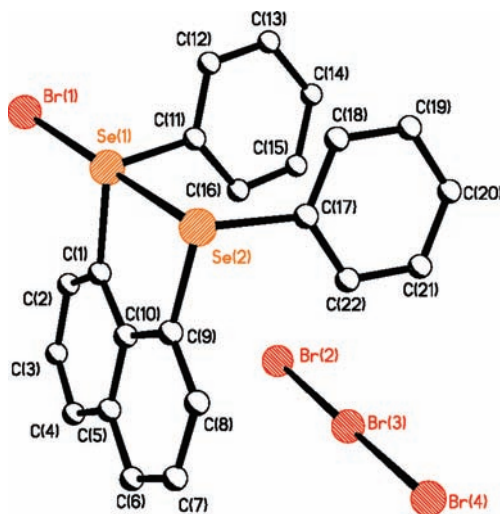


Figure 3. Molecular structure of the ionic CT “extended spoke” adduct 2 formed from the reaction of **D2** with dibromine (compound 3 adopts a similar structure, see the Supporting Information).

afford “T-shaped”/“seesaw” adducts with no tellurium CT “spoke” adducts having been reported.^{15,22} Tellurium forms a strong donor–strong acceptor system with dihalogen molecules sufficient to cleave the X–X bond and oxidize tellurium.^{15,22} Nucleophilic attack occurring at the chalcogen site of a diorganotellurium [$R_2\text{Te}-X$]⁺ cation affords a “seesaw” hypervalent adduct containing the quasi linear X–Te–X alignment.^{15,22}

Tellurium-donor compounds 1-(phenyltellurenyl)-8-(phenylsulfanyl)naphthalene **D4** and 1-(phenyltellurenyl)-8-(phenylselenyl)naphthalene **D5** react conventionally with dibromine and diiodine, affording a series of “seesaw” insertion adducts (Scheme 1). In all four reactions, the dihalogen reacts at the larger, less electronegative tellurium atom due to its greater electron donor ability over sulfur and selenium.^{43,48}

The formation of the X–Te–X fragment is confirmed by a significant downfield shift in the ¹²⁵Te NMR spectra for 7–10 compared to **D4** [$\delta = 715.2$ ppm]⁵⁷ and **D5** [$\delta = 687.6$ ppm].⁵⁷ Single peaks are observed in all four spectra with the signals for the bromine compounds 7 [$\delta = 958.9$ ppm] and 8 [$\delta = 941.4$ ppm] lying at expected higher chemical shifts compared to their iodine analogues 9 [$\delta = 790.9$ ppm] and 10 [$\delta = 747.0$ ppm]. A downfield shift is also observed in the ⁷⁷Se NMR spectra of 8 and 10 compared to **D5** [$\delta = 362.8$ ppm],⁵⁷ with single peaks at $\delta = 500.0$ ppm and $\delta = 428.8$ ppm, respectively.

The four adducts 7–10 are characterized by the well-known “seesaw” structure and incorporate an asymmetric linear X–Te–X fragment [7, 176.7(1)°; 8, 177.9(1)°; 9, 176.8(1)°; 10, 179.6(1)°] characterized by unequal X–Te bond lengths (Figure 8).²³ The central tellurium atom adopts a distorted trigonal bipyramidal (TBP) geometry with angles around tellurium for all four adducts in the range 87–98°. The formation of the linear fragment is accompanied by a minor adjustment to the naphthyl and phenyl ring conformations compared to the tellurium donor compounds **D4** and **D5**.⁵⁷ A slight rotation round the Te(1)–C(1) bond positions the Te–C_{Ph} bond intermediate between perpendicular and coplanar with the naphthyl plane, and both phenyl rings adopt twist conformations.⁶⁴ This affords a twist–twist and axial–twist arrangement corresponding to the “AC-type”

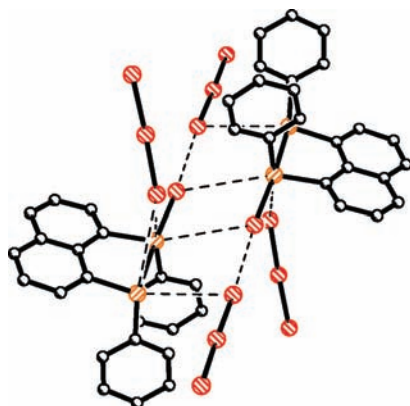


Figure 4. Intermolecular short contacts in the molecular structure of the ionic CT “extended spoke” adduct **2**, producing a quasi-linear rectangular arrangement of eight atoms.

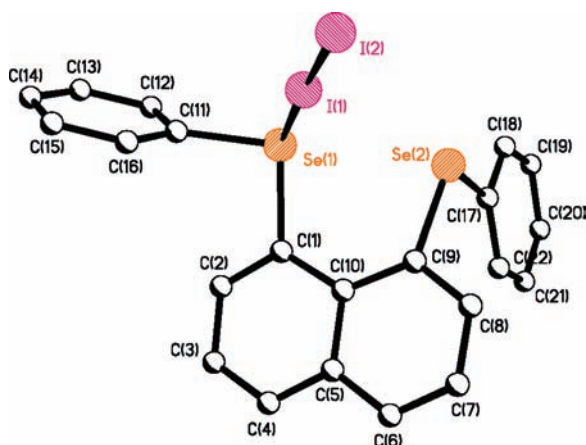
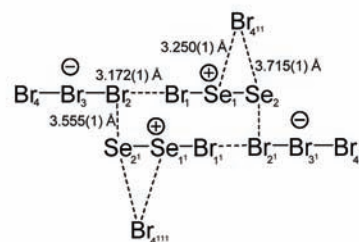


Figure 5. Molecular structure of the neutral CT “spoke” adduct **4**.

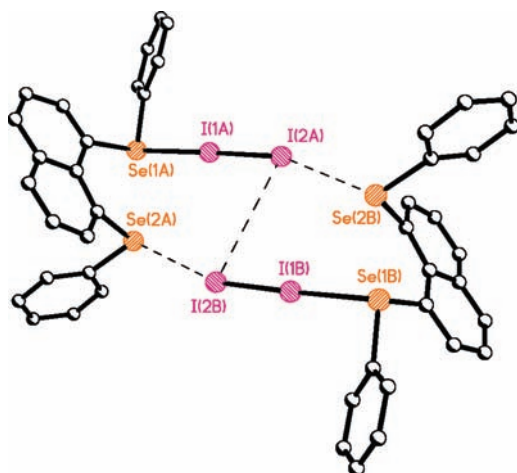


Figure 6. Intermolecular nonbonded short contacts between two neighboring molecules of adduct **4**.

structure (Figure 1).^{64,65} The alignment of the “seesaw” moiety positions one of the terminal halide atoms of X–Te–X in the *peri* gap and in close proximity to E(2). Noncovalent X···E(2) distances [7, 3.486(2) Å; 8, 3.542(2) Å; 9, 3.6136(16) Å; 10, 3.696(2) Å] are marginally shorter than the sum of van der Waals radii for the two interact-

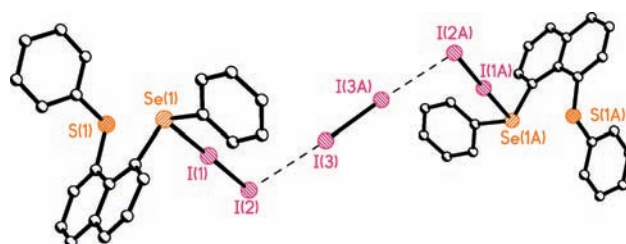


Figure 7. Molecular structure of the CT “extended spoke” adduct **6** characterized by a “Z-shaped” D–I₂···I₂···I₂–D system (adduct **5** adopts a similar structure, see the Supporting Information).

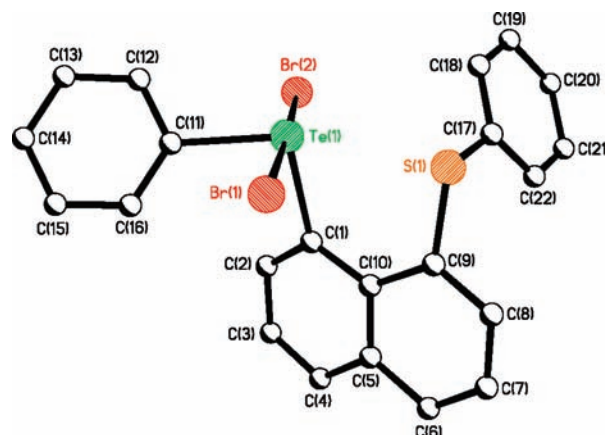


Figure 8. Molecular structure of the “seesaw” adduct **7** (adducts **8**–**10** display similar molecular structures, see the Supporting Information).

ing atoms [94–96%].⁶⁶ Te–Br [2.67–2.72 Å] and Te–I [2.89–2.95 Å] bond lengths are within the usual ranges [2.68, 2.99 ± 0.05 Å].⁷⁴

The naphthalene moieties of the “seesaw” adducts experience a similar degree of molecular distortion compared to donor compounds **D4** and **D5**.⁵⁷ As expected, the deformation of the naphthalene unit is greater in adducts **8** and **10** (TeSe) compared with compounds **7** and **9** (TeS). Intramolecular Te···S [7, 3.075(2) Å; 9, 3.0767(17) Å] and Te···Se [8, 3.141(2) Å; 10, 3.137(2) Å] *peri* distances are 20–22% shorter than the sum of van der Waals radii for the two chalcogen atoms and comparable to the separations in the independent molecules of **D4** [3.0684(13) Å (3.0984(11) Å)]⁵⁷ and **D5** [3.1919(11) Å (3.1580(12) Å)],⁵⁷ respectively. Deviation of the *peri* atoms within the naphthyl plane is marginally

(74) CSD Version 5.31, Conquest 1.12 & Vista. <http://www.ccdc.cam.ac.uk/> (accessed Jul 2010).

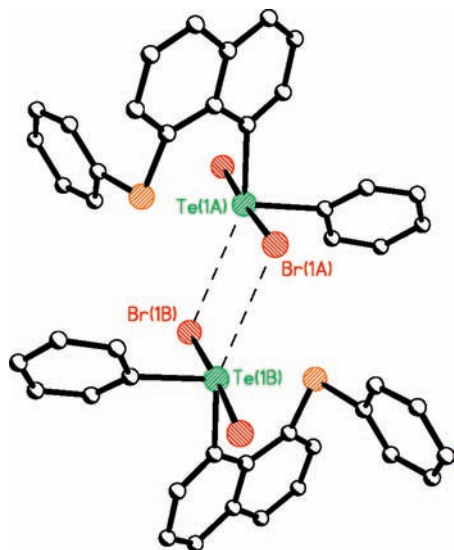


Figure 9. Short intermolecular contacts between neighboring molecules of the “T-shaped” adduct **7** form planar Te_2X_2 square units (**8**, **9**, and **10** adopt identical arrangements, see the Supporting Information).

greater in the selenium compounds **8** and **10** with large positive splay angles of the magnitude 13.5° and 12.4° [cf. 12.0° and 12.3° for **7** and **9**]. Distortion out-of-the plane is comparable throughout the series with atoms lying at distances between 0.3 and 0.4 Å, and the deviation of the central naphthalene ring torsion angles from planarity is also consistent, 0 – 7° . Short intermolecular contacts exist in each of the four adducts between Te and X atoms of neighboring molecules constructing planar Te_2X_2 squares (Figure 9). In all cases, the $\text{Te}\cdots\text{X}$ distance is 93–95% of the sum of van der Waals radii for the two interacting atoms.

The comparable reactions of 1-bromo-8-(phenyltellurenyl)naphthalene **D6** and 1-iodo-8-(phenyltellurenyl)naphthalene **D7** with dihalogens (Br_2 , I_2) afforded a similar array of “seesaw” insertion adducts **11**–**14** (Scheme 1). The ^{125}Te NMR spectra for **11**–**14** show a similar trend to that previously described for **7**–**10** with an expected downfield shift compared to their respective donor compounds **D6** [$\delta = 731.2$ ppm] 58 and **D7** [$\delta = 698.3$ ppm]. 58 Single peaks are observed in all spectra, with bromine compounds **11** [$\delta = 942.8$ ppm] and **12** [$\delta = 903.0$ ppm] possessing higher chemical shifts compared to their iodine counterparts **13** [$\delta = 887.5$ ppm] and **14** [$\delta = 848.0$ ppm].

Adducts **11**–**14** adopt similar “seesaw” geometries to those observed for **7**–**10**, but the linear $\text{X}-\text{Te}-\text{X}$ fragments are more symmetrical (Figure 10). Tellurium adopts a quasi-trigonal bipyramidal conformation with angles around the central atom in the range 87.4 – 99.4° . Adducts **11** and **12** containing Te and Br *peri* atoms adopt a twist–twist orientation of naphthyl and phenyl rings (“C-type”), while in adducts **13** and **14** (TeI) the $\text{Te}-\text{C}_{\text{Ph}}$ bond aligns along the naphthyl plane and the compounds display an equatorial–twist conformation (“B-type”; Figure 1). 64,65 The arrangement of the linear species in all four adducts positions one of the X atoms in the *peri* gap, but $\text{X}\cdots\text{X}'$ separations in all cases are greater than the sum of van der Waals radii for the two interacting halogen atoms. $\text{Te}-\text{Br}$ [2.66–2.68 Å] and $\text{Te}-\text{I}$ [2.90–2.95 Å] bond lengths are within the usual ranges [2.68, 2.99 ± 0.05 Å]. 74

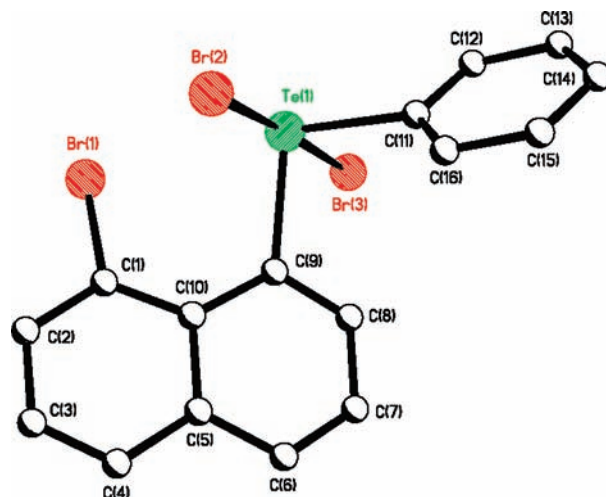


Figure 10. Molecular structure of the “seesaw” insertion adduct **11** (**12**–**14** adopt identical arrangements, see Supporting Information).

The substitution of bulky halogen atoms at the second *peri* position in **11**–**14** results in a greater degree of steric strain and consequently naphthalene distortion compared with adducts **7**–**10**. Additionally, the deformation of the naphthalene unit is greatest in adducts with an iodine *peri* atom, **12** and **14**, compared with **11** and **13** (Br). The intramolecular $\text{Te}\cdots\text{Br}$ *peri* distance in **11** [3.2397(15) Å] is larger than the separation in the tellurium donor compound **D6** [3.1909(10) Å], 58 while the distance in **13** is marginally shorter [3.1563(6) Å]. Conversely, the $\text{Te}\cdots\text{I}$ distances in **12** and **14** [3.3810(7) Å; 3.3608(11) Å] are longer than the separation in **D7** [3.3146(6) Å]. 58 In all cases, the $\text{Te}\cdots\text{X}$ separation is less than the sum of van der Waals radii for the two interacting atoms by 16–19%.

The increased congestion in the *peri* region of adducts **12** and **14** causes a larger divergence of the $\text{Te}-\text{C}$ and $\text{X}-\text{C}$ bonds within the naphthyl plane compared with **11** and **13**. Large positive splay angles are observed for all four adducts with those for **11** and **13** [13.1° ; 12.4°] similar in size to **D6** [13.6°] 58 and those for **12** and **14** [15.9° ; 18.7°] comparable to the splay in **D7** [16.2°]. 58 Adducts **11** and **12** containing the $\text{Br}-\text{Te}-\text{Br}$ linear fragment display the greatest out-of-plane distortion with atoms lying ~ 0.6 Å to opposite sides of the naphthalene least-squares plane. Adducts **11** and **12** also display a major distortion to the naphthalene ring system with maximum central naphthalene ring torsion angles of ~ 10 – 11° . Short intermolecular contacts between Te and I atoms of neighboring $\text{I}-\text{Te}-\text{I}$ units in **12** and **14** form similar planar Te_2X_2 square units to **7**–**10**. Although a number of short contacts exist in adducts **11** and **13**, no similar intermolecular arrangement is observed.

We have recently reported the synthesis and structural study of (8-phenylsulfanylnaphth-1-yl)diphenylphosphine **D8**; a complete series of phosphorus(V) oxygen, sulfur, and selenium chalcogenides; and a study of its coordination chemistry. 56 Treatment of **D8** with excess dibromine in dichloromethane led to the formation of the air-stable phosphonium salt **15**. Phosphorus forms a four-coordinate cationic fragment via the addition of a hydroxyl group which is balanced by a linear Br_3^- counteranion (Scheme 1). The ^{31}P NMR spectrum shows a single peak at $\delta = 52.48$ ppm.

The molecular structure of **15** is shown in Figure 11. In the asymmetric unit, two molecules of **15** share the proton

situated between the oxygen atoms and form a “Z-shaped” P–O–H–O–P bridge. All five atoms lie on the same plane with P–O–H angles of $131.2(1)^\circ$ and an O–H–O angle of $180.0(1)^\circ$. P–O bond lengths are identical in both molecules [$1.527(6)$ Å] with a value in between the observed P=O bond length in the phosphine oxide of **D8** (**D8=O**) [$1.492(2)$ Å]⁵⁶ and a standard single P–OH bond [1.56 Å].⁷⁵ This suggests that the structure is an average of a phosphine oxide and a phosphonium cation, as depicted in Figure 12. The charge of the cation is balanced by the presence of a linear Br₃[−] counteranion [$180.00(6)^\circ$], which exhibits elongated Br–Br bond lengths [$2.5984(12)$ Å] compared to free bromine [2.28 Å].⁴⁸

The naphthalene component of the phosphonium salt **15** exhibits greater strain relief and naphthalene distortion compared to phosphine **D8** and its phosphine oxide **D8=O**.⁵⁶ The *peri* atoms are accommodated by an intramolecular nonbonded P⋯S distance of $3.165(2)$ Å, notably larger than the separation in **D8** [$3.0330(7)$ Å] and **D8=O** [$3.1489(9)$ Å].⁵⁶ The divergence of the P–C and S–C bonds within the naphthyl plane is also more pronounced in **15**, with a large positive splay angle of 15.5° [cf. **D8**, 14.1 ; **D8=O**, 12.4].⁵⁶ Additionally, the *peri* atoms are displaced to opposite sides of the mean naphthalene by $0.436(11)$ Å (P) and $-0.466(11)$ Å (S). The naphthalene backbone in the phosphonium salt displays a significant deformation from planarity, with maximum C–C–C–C torsion angles lying in the range 5 – 8° . One short intramolecular S⋯O contact exists with a separation 11% shorter than the sum of van der Waals radii for the two atoms. Although a number of short intermolecular interactions exist, there is no significant overlap of phenyl or naphthyl rings and no π – π stacking is observed.

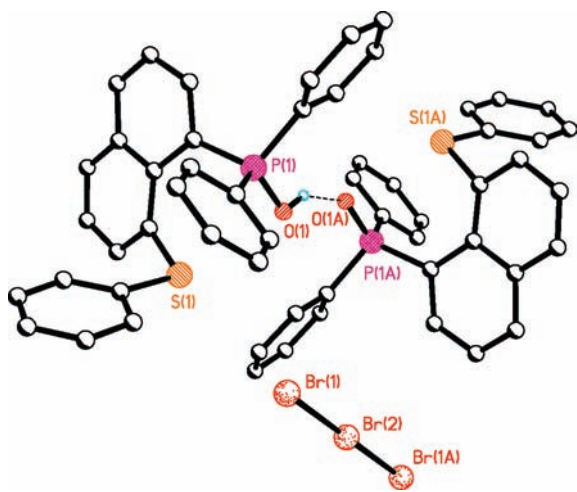


Figure 11. Molecular structure of hydroxydiphenyl[(8-phenylsulfonyl)naphthalene-1-yl]phosphonium tribromide **15**.

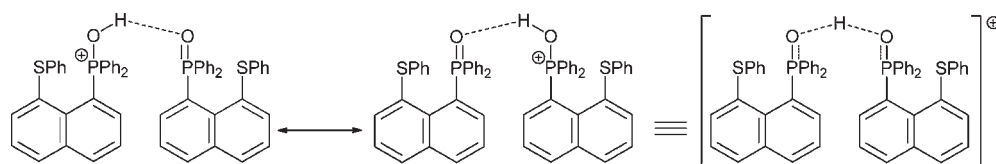


Figure 12. Crystal structure of **15**. Two molecules share a proton to form a P–O–H–O–P bridge, explained by an average structure of a phosphine oxide and a phosphonium cation.

3. DFT Calculations

Of the compounds presented here, only **2** and **3** display a reduction in naphthalene distortion and by inference the degree of steric strain operating between the *peri* atoms, compared with parent donor compounds (**D2** and **D3**).⁵⁷ This can be rationalized by the presence of an attractive weak interaction between the *peri* atoms, inferred by the noticeable shrinkage of the *peri* distance in both adducts. In addition, the two *peri* atoms align with one bromine atom to form a quasi-linear Br(1)–Se(1)⋯E(2) arrangement, suggesting the nature of the bonding could be represented by the 3c–4e mode. To try and assess the possibility of direct Se(1)⋯E(2) bonding interactions that would indicate an onset of 3c–4e bonding in **2** and **3**, density functional theory computations were performed for the possible reaction products between 1,8-(SePh)₂-C₁₀H₆ (**D2**) and Br₂, optimized at the B3LYP/962(+d)/6-31+G* level (Figure 13).

Structure **A** (Figure 13) corresponds to that observed in the solid for **2**; **A**⁺ is the isolated cationic fragment of this ion pair; **B** corresponds to the analogue where Se^a is replaced with Te (**8**) and **C** to that where Br is replaced with I (**4** and **5**). Optimizations starting from the two different conformations found in the latter two solids converged to the same minimum. Optimizations for **A** starting from the coordinates of **2** and its S-analogue **3** afforded two distinct minima, which differ in the exact position of the Br₃ moiety. Both are very close in energy, within *ca.* 1 kcal/mol, and only the results for the most stable conformer (derived from solid **3**) will be discussed in the following. As expected, the Se⋯Se contacts are shortest in **A** and **A**⁺, with substantial bonding interactions indicated by Wiberg bond indices (WBI)⁷⁶ of *ca.* 0.3–0.4. For comparison, the fully covalent S–S single bond in naphtho(1,8-cd)(1,2-dithiole) has a WBI of 0.99 at the same level. The optimized Se–Se distance for **A**, 2.807 Å, is in very good agreement with that observed in solid **2**, 2.762 Å, even though the Br₃ moiety has moved somewhat closer to the cationic fragment in the gas-phase optimization (Se^a⋯Br and Se^b⋯Br of 3.42 Å and 3.87 Å, respectively), as compared to the solid (where Se^a⋯Br and Se^b⋯Br are 3.55 Å and 4.40 Å, respectively). In **B** and **C**, the Se⋯Se distances are larger than in **A** and **A**⁺, and weaker but still noticeable bonding is found (WBI ≈ 0.1). The refined selenium–selenium distances for species **2** and **3** suggest that 3c–4e bonding is present in both cases.

Significant energetic driving forces are computed for all products **A**–**C** already in the gas phase (*cf.* the negative $\Delta E_r + \text{ZPE}$ values). The largest such driving force is computed for **A**, the actual, crystallized product, but compounds **B** and **C** are only a few kilocalories per mole less stable. Standard entropic and enthalpic corrections would reduce the free energy of bromination to essentially zero for **B** and **C** and would make formation of **A** endergonic (see $\Delta G_r^{298\text{K}}$ values). Immersion in a polarizable continuum favors the

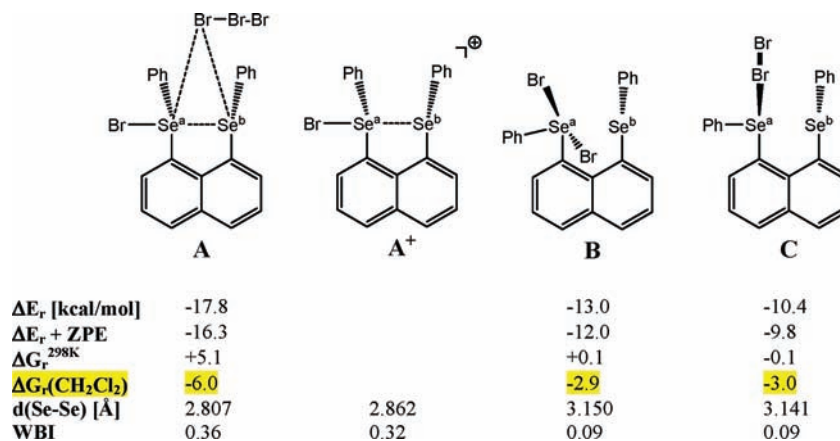


Figure 13. DFT computations performed at the B3LYP level for the possible reaction products between **D2** and Br_2 . ΔE_r , $\Delta E_r + \text{ZPE}$, and $\Delta G_r^{298\text{K}}$ are gas-phase relative energies, zero-point corrected energies, and free energies, respectively, relative to $\text{D2} + n\text{Br}_2$; $\Delta G_r(\text{CH}_2\text{Cl}_2)$ are free energies (at 298 K) corrected for solvation effects.

formation of **B** and **C** slightly, by *ca.* -3 kcal/mol, and stabilizes the highly polar ion pair **A** significantly, by *ca.* -11 kcal/mol. Judging from the $\Delta G_r(\text{CH}_2\text{Cl}_2)$ values, formation of all products is exergonic in a condensed phase, with a slight preference for the observed product **A**. These results therefore suggest that the occurrence of **A** may not be due to its intrinsic stability but would rather arise from its favorable interaction with the polar environment of the crystal. Notwithstanding the crude nature of some approximations involved (ideal-gas entropies, continuum solvation model), the relative free energies in solution are computed to be rather similar for all products. This would help to rationalize the rather diverse chemistry encountered upon varying the chalcogen and/or the halogen in this system.

Because the relative free energies of the various products appear to be rather closely spaced, it is conceivable that complex equilibria rather than a single product might occur in solution, and that, thus, the nature of the species present in solution could be different from that in the solid state. This is in agreement with the generally accepted mechanism to describe the formation of adducts from the reaction of diorganochalcogen donors with the dihalogens,^{14,38,39} in solution the CT “spoke” and the “seesaw” adducts of type $\text{RRE} \cdot \text{X}_2$ are in equilibrium, and as reported by Husebye and co-workers, all of the products in these reactions are derived from a common intermediate species $[\text{R}_2\text{E}-\text{X}]^+$.^{15,22,40}

4. Conclusions

The structural conformation of the products formed from the reactions between donor compounds **D1–D8** and the dihalogens is dependent on several factors, most importantly the donor ability of the chalcogen atom, the acceptor ability of the dihalogen species, and the stoichiometry of the reactants. When two donor atoms are available (**D3**, **D4**, **D5**), reaction occurs explicitly between the dihalogen and the least electronegative element. The neutral charge-transfer (CT) “spoke” adduct and the “seesaw” insertion adduct, characteristic of quasi-linear hypervalent $\text{E}-\text{X}-\text{Y}$ ^{15,22,28,34,35} and $\text{X}-\text{E}-\text{Y}$ ^{14,15,22,28,31,36,37} fragments, respectively, are the most common structural motifs generated from the reaction of

diorganochalcogen donors $[\text{R}_2\text{E}]$ with inter- or dihalogens.^{15,22} In general, the reactions between **D1–D8** and the dihalogens conform to the charge-transfer rule and form “seesaw” adducts when the halogen (X) species is more electronegative than the chalcogen donor (E) $[\text{R}_2\text{E}^{\delta+}-\text{X}^{\delta-}]$ and form CT “spoke” adducts if the converse is true.^{20–22}

Reactions between Te donors $[\chi(\text{Te}) 2.08]$ ⁴³ and any dihalogen $[\chi(\text{F}) 3.94, \chi(\text{I}) 2.36]$ ⁴³ explicitly afford “seesaw” or “T-shaped” adducts with no CT adducts known for any tellurium compound.^{14,15,22,43} Tellurium donor compounds **D4–D7** react conventionally to form strong donor–strong acceptor systems with the dihalogens. The X–X bond is cleaved, and the Te atom is oxidized.^{14,15,22} In each case, nucleophilic attack occurs at the tellurium site of the $[\text{R}_2\text{Te}-\text{X}]^+$ cation, affording a series of “seesaw” hypervalent adducts **7–14** characterized by the quasi-linear X–Te–X alignment.^{14,15,22}

As expected from electronegativity values, all structurally reported adducts formed from the reaction of diorganoselenium compounds $[\chi(\text{Se}) 2.35]$ ⁴³ with dibromine $[\chi(\text{Br}) 2.58]$ ⁴³ adopt the “seesaw” geometry.^{14,15,22,47,49,50} The decrease in the electronegativity difference between selenium and iodine $[\chi(\text{Br}) 2.36]$ ⁴³ favors the formation of CT “spoke” adducts.^{15,22,46,47} The selenium-donor compounds **D2** and **D3** react to form strong donor–strong acceptor systems with dibromine sufficient to cleave the Br–Br bond and oxidize the selenium atom.^{15,22} The hypervalent 3c–4e interaction operating between the quasi-linear $\text{Br}-\text{Se} \cdots \text{E}$ arrangement in both compounds blocks the nucleophilic attack at the selenium site of the $[\text{R}_2\text{Se}-\text{X}]^+$ cation, so no “seesaw” adduct is formed. Instead, a hypervalent linear tribromide counteranion balances the charge, and the ionic tribromide salts **2** and **3** are formed, which can be represented by the formula $[\text{RSe}-\text{Br}]^+ \cdots [\text{Br}-\text{Br}_2]^{-2}$.³⁴

D2 reacts conventionally with a single equivalent of diiodine to form the CT “spoke” adduct **4** characterized by the quasi-linear $\text{Se}-\text{I}-\text{I}$ alignment. Reaction with a higher equivalent of diiodine (1:2) affords a structurally more complex “extended spoke” adduct **5**, incorporating I_2 chains. Two molecules of adduct **4** acting as donors interact with a single bridging diiodine molecule via soft–soft $\text{I} \cdots \text{I}$ interactions to construct a “Z-shaped” system with a $\text{D}-\text{I}_2 \cdots \text{I}_2 \cdots \text{I}_2-\text{D}$ configuration. **D3** reacts to form a comparable system, **6**. These “Z-shaped” systems are of great interest, as

(75) Allen, F. H.; Kennard, O.; Watson, D. G.; Brammer, L.; Orpen, A. G.; Taylor, R. *J. Chem. Soc., Perkin Trans. 2* **1987**, S1.

(76) Wiberg, K. B. *Tetrahedron* **1968**, *24*, 1083.

compounds with extended poly(I₂) chains held by weak I₂···I₂ interactions and also adducts formed with a donor/dihalogen composition greater than 1:1 are extremely rare.^{15,71}

Adducts formed from the reaction of organosulfur compounds with dibromine are rare.^{15,22,28,42,51} Resonance lone pairs on sulfur in **D1** and **D8** are delocalized into the aromatic π system, reducing the donor ability of the compound for reaction with the dihalogens. The aromatic groups in **D1** are strongly activated and highly reactive toward electrophilic substitution.⁵⁹ Upon treatment with dibromine, **D1** undergoes a standard electrophilic aromatic substitution reaction which substitutes bromine atoms in the 4 and 8 positions on the naphthyl ring and in the *para* positions on the two phenyl rings. Phosphine **D8** neither reacts to form an adduct nor undergoes electrophilic aromatic substitution. Instead, treatment with dibromine affords the tetravalent phosphonium salt **15**, which packs via a “Z-shaped” P–O–H–O–P bridge and is charge-balanced by the presence of a tribromide counteranion.

Aragoni et al. have recently reviewed the nature of the bonding in linear three-body systems including the E–X–X and X–E–X arrangements of the CT “spoke” and “seesaw” adducts.²³ They concluded that these linear moieties can be accounted for by a charge-transfer model and the three-center, four-electron bond (3c–4e) model introduced by Rundle and Pimentel to explain the hypervalency in the trihalide ions.^{7,11} The linear three-body systems present in **2–14** conform to the 3c–4e model and as such have weaker and, by inference, longer bond lengths compared with the distances between atoms in standard single electron pair 2c–2e bonds. The tribromide anions present in compounds **2**, **3**, and **15** all display elongated Br–Br bond distances [2.52–2.60 Å] compared to free dibromine [2.28 Å]⁴⁸ but within the usual range for Br₃[–] ions [2.5–2.6 Å].⁷⁴ Similarly, I–I bond lengths exhibit a noticeable lengthening in the Se–I–I fragments of compounds **4–6** [2.80–2.87 Å] compared with free diiodine [2.66 Å].⁴⁸ Te–Br and Te–I bond lengths in the linear Br–Te–Br and I–Te–I fragments of the “seesaw” insertion adducts **7–14** are within the usual range.²³

Following treatment with dibromine and diiodine, the degree of distortion and, by inference, the steric strain operating between the *peri* atoms in their addition products **2–15** (and the substitution product **1**) in general appears unchanged. The exceptions to this are the two tribromide salts of bromoselenyl cations (**2**, **3**), which display a reduction in the distortion of the naphthalene geometry compared to parent donor compounds **D2** and **D3**, respectively. This can be rationalized by the existence of the quasi-linear Br(1)–Se(1)···E(2) interaction in both compounds, which can be represented by the 3c–4e model. The attractive weak interaction between the *peri* atoms, inferred by the noticeable shrinkage of the *peri* distance in both adducts, reduces the steric hindrance and therefore the required distortion of the naphthalene scaffold. From DFT calculations performed on **2**, the optimized Se–Se distance [2.746 Å] is in excellent agreement with that observed in the solid [2.762 Å], and the WBI value⁷⁶ of 0.4 indicates a considerable bonding interaction and the onset of 3c–4e bonding in the quasi-linear three-body system.

5. Experimental Section

All experiments were carried out under an oxygen- and moisture-free nitrogen atmosphere using standard Schlenk

techniques and glassware. Reagents were obtained from commercial sources and used as received. Dry solvents were collected from an MBraun solvent system. Elemental analyses were performed by the University of St. Andrews School of Chemistry Microanalysis Service. Infrared spectra were recorded as KBr discs in the range 4000–300 cm^{–1} on a Perkin-Elmer System 2000 Fourier transform spectrometer. ¹H and ¹³C NMR spectra were recorded on a Jeol GSX 270 MHz spectrometer with δ (H) and δ (C) referenced to external tetramethylsilane. ³¹P, ⁷⁷Se, and ¹²⁵Te NMR spectra were recorded on a Jeol GSX 270 MHz spectrometer with δ (P), δ (Se), and δ (Te) referenced to external phosphoric acid, dimethylselenide, and diphenyl ditelluride, respectively. Assignments of ¹³C and ¹H NMR spectra were made with the help of H–H COSY and HSQC experiments. All measurements were performed at 25 °C. All values reported for NMR spectroscopy are in parts per million (ppm). Coupling constants (*J*) are given in Hertz (Hz). Mass spectrometry was performed by the University of St. Andrews Mass Spectrometry Service. Electron impact mass spectrometry (EIMS) and chemical ionization mass spectrometry (CIMS) were carried out on a Micromass GCT orthogonal acceleration time-of-flight mass spectrometer. Electro spray mass spectrometry (ESMS) was carried out on a Micromass LCT orthogonal accelerator time-of-flight mass spectrometer.

1,8-Bis(4-bromophenylsulfanyl)-2,5-dibromonaphthalene (1). A solution of 1,8-diphenylsulfanylnaphthalene, **D1** (0.22 g, 0.63 mmol), in dichloromethane (20 mL) was cooled to 0 °C and slowly treated with bromine (0.2 g, 0.06 mL, 1.3 mmol). An analytically pure sample was obtained by crystallization from the diffusion of pentane into a dichloromethane solution of the product (0.3 g, 75%). Anal. Found: C, 41.2; H, 1.8. Calcd for C₂₂H₁₂S₂Br₄: C, 40.3; H, 1.8%. ν_{\max} (KBr disk)/cm^{–1}: 3401w, 3075w, 2920w, 2848w, 2362w, 1881w, 1570s, 1558s, 1470vs, 1400w, 1382s, 1320w, 1282s, 1268s, 1185s, 1083s, 1065s, 1018w, 1006vs, 805vs, 765w, 745s, 688w, 641w, 608w, 561w, 517w, 497w, 471s, 417w, 396w, 373w, 352w. δ_{H} (270 MHz, CDCl₃): 8.19 (1 H, d, *J* 9.1 Hz, *nap* 4-H), 7.80 (1 H, d, *J* 9.1 Hz, *nap* 3-H), 7.46 (1 H, d, *J* 8.2 Hz, *nap* 6-H), 7.33 (2 H, d, *J* 8.4 Hz, *SPhBr* 3,5-H), 7.21 (2 H, d, *J* 8.6 Hz, *SPhBr* 9,11-H), 7.05 (2 H, d, *J* 8.4 Hz, *SPhBr* 2,6-H), 6.95 (1 H, d, *J* 8.2 Hz, *nap* 2-H), 6.74 (2 H, d, *J* 8.6 Hz, *SPhBr* 8,12-H). δ_{C} (67.9 MHz, CDCl₃): 135.4(s), 132.9(s), 132.5(s), 132.1(s), 131.8(s), 130.7(s), 128.3(s). *m/z* (EI⁺) 659.69 ([M]⁺, 100%), 347.80 ([M – 2(ArBr)]⁺, 98%).

Compound 2. A solution of 1,8-bis(phenylselenenyl)naphthalene, **D2** (0.21 g, 0.47 mmol), in dichloromethane (20 mL) was cooled to 0 °C and slowly treated with bromine (0.15 g, 0.05 mL, 0.93 mmol). An analytically pure sample was obtained by crystallization from the diffusion of dichloromethane into a pentane solution of the product (0.2 g, 57%). Anal. Found: C, 39.6; H, 1.3. Calcd for C₂₂H₁₆Se₂Br₄: C, 40.3; H, 2.5%. ν_{\max} (KBr disk)/cm^{–1}: 3396w, 3050w, 2920w, 2848w, 2356w, 2325w, 1589w, 1566w, 1486s, 1470s, 1438s, 1346s, 1261w, 1212w, 1194w, 1176w, 1083w, 1047s, 1016w, 992s, 825s, 812vs, 757w, 744vs, 730vs, 679vs, 659w, 533w, 484w, 463s, 457s, 442w, 378w. *m/z* (ES⁺) 539.11 ([M – Br₃ + Na]⁺, 100%).

Compound 3. A solution of 1-(phenylselenenyl)-8-(phenylsulfanyl)naphthalene, **D3** (0.02 g, 0.051 mmol), in dichloromethane (5 mL) was cooled to 0 °C and slowly treated with bromine (0.02 g, 0.005 mL, 0.10 mmol). An analytically pure sample was obtained by crystallization from the diffusion of dichloromethane into a pentane solution of the product (0.01 g, 33%). ν_{\max} (KBr disk)/cm^{–1}: 3447vs, 3418vs, 2924vs, 2848s, 2372w, 1985w, 1918w, 1773w, 1735s, 1718s, 1703s, 1686s, 1654s, 1636s, 1578s, 1543s, 1523w, 1459s, 1436s, 1383w, 1343w, 1261w, 1203w, 1177w, 1148w, 1087s, 1020w, 913w, 814vs, 751vs, 735vs, 692w, 602w, 541w, 456s, 398w. *m/z* (ES⁺): 422.83 ([M – Br₄ + OMe]⁺, 97%), 391.83 ([M – Br₄]⁺, 100%).

Compound **4**. A solution of 1,8-bis(phenylselenyl)naphthalene, **D2** (0.23 g, 0.53 mmol), in dichloromethane (20 mL) was cooled to 0 °C and slowly treated with iodine (0.13 g, 0.53 mmol). An analytically pure sample was obtained by crystallization from the diffusion of dichloromethane into a pentane solution of the product (0.2 g, 66%). Anal. Found: C, 39.5; H, 2.2. Calcd for $C_{22}H_{16}Se_2I_2$: C, 38.2; H, 2.3%. ν_{max} (KBr disk)/ cm^{-1} : 3406w, 3050w, 2920w, 2848w, 2382w, 1690w, 1659w, 1573s, 1550w, 1473s, 1435s, 1331w, 1191w, 1137w, 1088w, 1060s, 1018s, 995w, 956w, 912w, 838w, 811vs, 750s, 737vs, 687vs, 662s, 613w, 471w, 453w. δ_H (270 MHz, $CDCl_3$): 7.82 (2 H, dd, J 1.0 and 8.2 Hz, nap 4,5-H), 7.72 (2 H, dd, J 1.2 and 7.4 Hz, nap 2,7-H), 7.47–7.37 (4 H, m, *SePh* 2,6-H), 7.36–7.20 (8 H, m, nap 3,6-H, *SePh* 3–5-H). δ_C (67.9 MHz, $CDCl_3$): 136.2(s), 133.1(s), 130.1(s), 129.7(s), 128.0(s), 126.4(s). δ_{Se} (51.5 MHz, $CDCl_3$): 436.9, 436.7. m/z (ES^+): 565.99 ($[M - I]^+$, 5%), 440.12 ($[M - I_2]^+$, 100%).

Compound **5**. A solution of compound **4** (0.24 g, 0.35 mmol) in dichloromethane (20 mL) was cooled to 0 °C and slowly treated with iodine (0.09 g, 0.35 mmol). An analytically pure sample was obtained by crystallization from the diffusion of dichloromethane into a pentane solution of the product. δ_H (270 MHz, $CDCl_3$): 7.74 (2 H, dd, J 1.0 and 8.2 Hz, nap 4,5-H), 7.63 (2 H, dd, J 1.2 and 7.4 Hz, nap 2,7-H), 7.44–7.37 (4 H, m, *SePh* 2,6-H), 7.28–7.20 (8 H, m, nap 3,6-H, *SePh* 3–5-H). δ_{Se} (51.5 MHz, $CDCl_3$): 445.1, 444.3.

Compound **6**. A solution of 1-(phenylselenyl)-8-(phenylsulfanyl)naphthalene, **D3** (0.066 g, 0.17 mmol), in dichloromethane (5 mL) was treated with iodine (0.086 g, 0.34 mmol). An analytically pure sample was obtained by crystallization from the diffusion of dichloromethane into a pentane solution of the product (0.07 g, 18%). Anal. Found: C, 34.6; H, 2.1. Calcd for $(C_{22}H_{16}SSe_2)I$: C, 34.2; H, 2.1%. ν_{max} (KBr disk)/ cm^{-1} : 3434brs, 3040w, 1940w, 1880w, 1803w, 1720w, 1655w, 1575s, 1541w, 1473s, 1435s, 1350w, 1324s, 1301w, 1196s, 1139w, 1059w, 1019s, 996s, 968w, 900w, 815vs, 783s, 754s, 737vs, 687vs, 615w, 540w, 520w, 483w, 455s. δ_H (270 MHz, $CDCl_3$): 7.98–7.89 (2 H, m, nap 2,4-H), 7.76 (1 H, dd, J 1.9 and 7.2 Hz, nap 5-H), 7.68–7.60 (2 H, m, *SePh* 2,6-H), 7.50 (1 H, t, J 7.7 Hz, nap 3-H), 7.43–7.33 (3 H, m, *SePh* 3–5-H), 7.28–7.15 (4 H, m, nap 6-H, *SPh* 3–5-H), 7.15–7.06 (1 H, m, nap 7-H), 7.06–6.97 (2 H, m, *SPh* 2,6-H). δ_C (67.9 MHz, $CDCl_3$): 139.2(s), 135.9(s), 132.3(s), 131.7(s), 131.6(s), 130.1(s), 129.6(s), 129.2(s), 127.4(s), 126.5(s), 126.4(s), 126.0(s). δ_{Se} (51.5 MHz, $CDCl_3$): 476.9. m/z (ES^+): 391.89 ($[M - I_2]^+$, 100%).

Compound **7**. A solution of 1-(phenyltellurenyl)-8-(phenylsulfanyl)naphthalene, **D4** (0.032 g, 0.073 mmol), in dichloromethane (5 mL) was treated with bromine (0.023 g, 0.007 mL, 0.15 mmol). An analytically pure sample was obtained by crystallization from the diffusion of dichloromethane into a pentane solution of the product (0.04 g, 80%). Anal. Found: C, 42.6; H, 2.7. Calcd for $C_{22}H_{16}TeSBr_2$: C, 44.0; H, 2.7%. ν_{max} (KBr disk)/ cm^{-1} : 3441brs, 3052w, 2953w, 1944w, 1869w, 1578s, 1475s, 1437s, 1325w, 1261w, 1200w, 1180w, 1072w, 1049w, 1046w, 1023w, 991s, 907w, 814vs, 757vs, 738s, 726vs, 680vs, 619w, 564w, 538w, 480w, 448s. δ_H (270 MHz, $CDCl_3$): 8.26–7.96 (6 H, m, nap 2,4,5,7-H, *TePh* 2,6-H), 7.70–7.40 (5 H, m, nap 3,6-H, *TePh* 3–5-H), 7.32–7.00 (5 H, m, *SPh* 2–6-H); δ_C (67.9 MHz, $CDCl_3$): 139.7(s), 138.1(s), 134.3(s), 133.5(s), 132.5(s), 131.5(s), 130.3(s), 130.1(s), 129.6(s), 128.8(s), 127.4(s), 127.3(s). δ_{Te} (81.2 MHz, $CDCl_3$): 958.9. m/z (ES^+): 472.79 ($[M - Br_2 + OMe]^+$, 100%).

Compound **8**. A solution of 1-(phenyltellurenyl)-8-(phenylselenyl)naphthalene, **D5** (0.12 g, 0.24 mmol), in dichloromethane (5 mL) was treated with bromine (0.038 g, 0.01 mL, 0.24 mmol). An analytically pure sample was obtained by crystallization from the diffusion of dichloromethane into a pentane solution of the product (0.1 g, 75%). Anal. Found: C, 40.7; H, 2.0. Calcd for $C_{22}H_{16}TeSeBr_2$: C, 40.9; H, 2.5%. ν_{max} (KBr disk)/ cm^{-1} : 3441brs, 3052s, 1944w, 1869w, 1738w, 1721w,

1651w, 1604w, 1572s, 1535w, 1475s, 1436s, 1378w, 1331s, 1209w, 1195w, 1177w, 1136w, 1081w, 1064w, 1049s, 1020w, 994s, 907w, 813vs, 755vs, 727vs, 680s, 613w, 555w, 526w, 446s, 314w. δ_H (270 MHz, $CDCl_3$): 8.32 (2 H, d, J 7.0 Hz, *TePh* 2,6-H), 8.28 (1 H, d, J 7.2 Hz, nap 4-H), 8.21 (1 H, d, J 7.3 Hz, nap 5-H), 8.09 (1 H, d, J 7.6 Hz, nap 7-H), 8.05 (1 H, d, J 7.7 Hz, nap 2-H), 7.64–7.44 (5 H, m, nap 3,6-H, *TePh* 3–5-H), 7.36–7.29 (2 H, m, *SePh* 2,6-H), 7.24–7.17 (3 H, m, *SePh* 3–5-H). δ_C (67.9 MHz, $CDCl_3$): 141.1(s), 138.8(s), 136.7(s), 133.6(s), 132.3(s), 131.3(s), 130.7(s), 129.9(s), 129.6(s), 127.7(s), 127.2(s), 126.9(s). δ_{Se} (51.5 MHz, $CDCl_3$): 500.0. δ_{Te} (81.2 MHz, $CDCl_3$): 941.4. m/z (ES^+): 518.69 ($[M - Br_2 + OMe]^+$, 100%).

Compound **9**. A solution of 1-(phenyltellurenyl)-8-(phenylsulfanyl)naphthalene, **D4** (0.032 g, 0.073 mmol), in dichloromethane (5 mL) was treated with iodine (0.018 g, 0.073 mmol). An analytically pure sample was obtained by crystallization from the diffusion of dichloromethane into a pentane solution of the product (0.04 g, 80%). ν_{max} (KBr disk)/ cm^{-1} : 3448brs, 3045w, 2920w, 2371w, 2342w, 1720w, 1686w, 1652w, 1635w, 1578w, 1541w, 1524w, 1509w, 1475s, 1432s, 1381w, 1324s, 1261w, 1196w, 1156w, 1136w, 1073w, 1045w, 1022w, 991w, 928w, 905w, 813vs, 755vs, 734s, 723vs, 681vs, 617w, 563w, 535w, 478w, 446s, 350w. δ_H (270 MHz, $CDCl_3$): 8.37 (1 H, dd, J 0.6 and 7.5 Hz, nap 4-H), 8.22 (2 H, d, J 7.5 Hz, *TePh* 2,6-H), 8.17 (1 H, d, J 7.2 Hz, nap 2-H), 8.13–8.04 (2 H, m, nap 5,7-H), 7.66 (1 H, t, J 7.8 Hz, nap 6-H), 7.59–7.48 (2 H, m, nap 3-H, *TePh* 4-H), 7.43–7.34 (2 H, m, *TePh* 3,5-H), 7.23–7.15 (3 H, m, *SPh* 3–5-H), 7.05–6.97 (2 H, m, *SPh* 2,6-H). δ_C (67.9 MHz, $CDCl_3$): 140.1(s), 139.3(s), 138.2(s), 133.5(s), 132.6(s), 131.4(s), 130.1(s), 129.7(s), 128.1(s), 127.8(s), 127.6(s), 127.5(s). δ_{Te} (81.2 MHz, $CDCl_3$): 790.9. m/z (ES^+): 470.86 ($[M - I_2 + OMe]^+$, 100%).

Compound **10**. A solution of 1-(phenyltellurenyl)-8-(phenylselenyl)naphthalene, **D5** (0.13 g, 0.26 mmol), in dichloromethane (5 mL) was treated with iodine (0.065 g, 0.26 mmol). An analytically pure sample was obtained by crystallization from the diffusion of dichloromethane into a pentane solution of the product (0.2 g, 85%). Anal. Found: C, 36.0; H, 1.7. Calcd for $C_{22}H_{16}TeSe_2$: C, 35.7; H, 2.2%. ν_{max} (KBr disk)/ cm^{-1} : 3441brs, 3046w, 2273w, 1572w, 1474s, 1434s, 1328s, 1189w, 1064w, 1046w, 1017w, 991w, 834w, 810vs, 752vs, 722vs, 680vs, 610w, 523w, 438s, 314w. δ_H (270 MHz, $CDCl_3$): 8.12 (1 H, d, J 7.0 Hz, nap 4-H), 8.04 (1 H, d, J 8.1 Hz, nap 2-H), 8.00 (2 H, d, J 7.5 Hz, *TePh* 2,6-H), 7.68 (1 H, d, J 7.3 Hz, nap 5-H), 7.58 (2 H, d, J 7.4 Hz, nap 3,7-H), 7.49–7.43 (1 H, m, *TePh* 4-H), 7.42–7.32 (4 H, m, *TePh* 3,5-H, *SePh* 2,6-H), 7.22–7.16 (4 H, m, nap 6-H, *SePh* 3–5-H). δ_C (67.9 MHz, $CDCl_3$): 139.2(s), 135.7(s), 135.6(s), 133.4(s), 132.5(s), 131.6(s), 130.5(s), 129.5(s), 129.3(s), 127.7(s), 127.5(s), 126.1(s). δ_{Se} (51.5 MHz, $CDCl_3$): 428.8. δ_{Te} (81.2 MHz, $CDCl_3$): 747.0. m/z (ES^+): 518.66 ($[M - I_2 + OMe]^+$, 100%).

Compound **11**. A solution of 1-bromo-8-(phenyltellurenyl)naphthalene, **D6** (0.10 g, 0.25 mmol), in dichloromethane (5 mL) was treated with a 0.1 M solution of bromine in dichloromethane (0.25 mmol, 2.5 mL). An analytically pure sample was obtained by crystallization from the diffusion of dichloromethane into a pentane solution of the product (0.1 g, 91%). Anal. Found: C, 33.9; H, 2.2. Calcd for $C_{16}H_{11}TeBr_3$: C, 33.7; H, 2.0%. ν_{max} (KBr disk)/ cm^{-1} : 3424brs, 3051w, 2920w, 1655w, 1589w, 1569w, 1535w, 1470s, 1432s, 1330s, 1260s, 1186s, 1133w, 1048s, 993w, 945w, 917w, 897w, 806vs, 735vs, 681s, 453s. δ_H (270 MHz, $CDCl_3$): 8.45 (2 H, d, J 6.6 Hz, *TePh* 2,6-H), 8.08 (1 H, d, J 6.7 Hz, nap 5-H), 8.01 (2 H, d, J 7.5 Hz, nap 4,7-H), 7.91 (1 H, d, J 7.9 Hz, nap 2-H), 7.70–7.51 (3 H, m, *TePh* 3–5-H), 7.51–7.36 (2 H, m, nap 3,6-H). δ_C (67.9 MHz, $CDCl_3$): 137.2(s), 134.3(s), 133.5(s), 132.0(s), 130.2(s), 127.4(s), 126.9(s). δ_{Te} (81.2 MHz, $CDCl_3$): 942.8. m/z (ES^+): 442.76 ($[M - Br_2 + OMe]^+$, 100%).

Compound **12**. A solution of 1-iodo-8-(phenyltellurenyl)naphthalene, **D7** (0.09 g, 0.20 mmol), in dichloromethane

(5 mL) was cooled to 0 °C and slowly treated with a 0.1 M solution of bromine in dichloromethane (2.0 mL, 0.20 mmol). An analytically pure sample was obtained by crystallization from the diffusion of dichloromethane into a pentane solution of the product (0.1 g, 86%). ν_{\max} (KBr disk)/ cm^{-1} : 3449br s, 3045w, 2954s, 2924s, 2851w, 1561w, 1532w, 1467w, 1432s, 1324w, 1260s, 1182w, 1094w, 1019w, 991w, 937w, 902w, 871w, 805vs, 766w, 746w, 731vs, 697w, 680s, 643w, 560w, 520w, 501w, 452s, 387w. δ_{H} (270 MHz, CDCl_3): 8.41–8.29 (3 H, m, nap 4-H, *TePh* 2,6-H), 8.12 (1 H, d, *J* 7.2 Hz, nap 5-H), 7.96 (1 H, d, *J* 8.0 Hz, nap 7-H), 7.92 (1 H, d, *J* 7.4 Hz, nap 2-H), 7.63–7.46 (3 H, m, *TePh* 3–5-H), 7.38 (1 H, t, *J* 7.7 Hz, nap 6-H), 7.28 (1 H, t, *J* 7.7 Hz, nap 3-H). δ_{C} (67.9 MHz, CDCl_3): 142.2(s), 138.6(s), 137.2(s), 133.9(s), 131.8(s), 130.9(s), 130.1(s), 127.9(s), 126.6(s). δ_{Te} (81.2 MHz, CDCl_3): 903.0. m/z (ES^+): 488.71 ($[\text{M} - \text{Br}_2 + \text{OMe}]^+$, 100%).

Compound **13**. A solution of 1-bromo-8-(phenyltellurenyl)naphthalene, **D6** (0.039 g, 0.095 mmol), in dichloromethane (5 mL) was treated with iodine (0.0024 g, 0.095 mmol). An analytically pure sample was obtained by crystallization from the diffusion of dichloromethane into a pentane solution of the product (0.03 g, 54%). ν_{\max} (KBr disk)/ cm^{-1} : 3433br s, 3040w, 2925w, 2371w, 1652w, 1638w, 1561w, 1532w, 1467s, 1432s, 1381w, 1327w, 1259w, 1207w, 1184w, 1130w, 1045s, 991w, 942w, 911w, 825w, 805vs, 746s, 729s, 680s, 603w, 526w, 446s, 432w. δ_{H} (270 MHz, CDCl_3): 8.48 (2 H, dd, *J* 1.1 and 8.5 Hz, *TePh* 2,6-H), 8.15 (1 H, dd, *J* 1.1 and 7.7 Hz, nap 4-H), 8.07 (2 H, m, nap 2,5-H), 7.92 (1 H, dd, *J* 0.8 and 8.3 Hz, nap 7-H), 7.67–7.59 (1 H, m, *TePh* 4-H), 7.53–7.42 (3 H, m, nap 6-H, *TePh* 3,5-H), 7.40 (1 H, t, *J* 7.8 Hz, nap 3-H). δ_{C} (67.9 MHz, CDCl_3): 139.7(s), 138.5(s), 134.2(s), 133.3(s), 131.8(s), 130.3(s), 130.1(s), 127.5(s), 127.1(s). δ_{Te} (81.2 MHz, CDCl_3): 887.5. m/z (ES^+): 442.76 ($[\text{M} - \text{I}_2 + \text{OMe}]^+$, 100%).

Compound **14**. A solution of 1-iodo-8-(phenyltellurenyl)naphthalene, **D7** (0.11 g, 0.25 mmol), in dichloromethane (5 mL) was treated with iodine (0.063 g, 0.25 mmol). An analytically pure sample was obtained by crystallization from the diffusion of dichloromethane into a pentane solution of the product (0.1 g, 81%). Anal. Found: C, 27.5; H, 1.3. Calcd for $\text{C}_{16}\text{H}_{11}\text{TeI}_3$: C, 26.9; H, 1.6%. ν_{\max} (KBr disk)/ cm^{-1} : 3430br s, 2959s, 2924vs, 2853s, 1735w, 1654w, 1529w, 1465w, 1430w, 1375w, 1363w, 1317w, 1261vs, 1177w, 1090vs, 1020vs, 866w, 802vs, 747w, 727w, 680w, 663w, 587w, 561w, 535w, 520w, 448w, 389w. δ_{H} (270 MHz, CDCl_3): 8.38–8.29 (2 H, m, *TePh* 2,6-H), 8.27 (1 H, dd, *J* 1.1 and 7.4 Hz, nap 4-H), 8.15 (1 H, dd, *J* 1.0 and 7.6 Hz, nap 5-H), 7.93 (1 H, d, *J* 8.1 Hz, nap 7-H), 7.86 (1 H, dd, *J* 1.0 and 8.2 Hz, nap 2-H), 7.57–7.49 (1 H, m, *TePh* 4-H), 7.44–7.34 (2 H, m, *TePh* 3,5-H), 7.30 (1 H, t, *J* 7.8 Hz, nap 6-H), 7.23 (1 H, t, *J* 7.8 Hz, nap 3-H). δ_{C} (67.9 MHz, CDCl_3): 142.1(s), 140.0(s), 139.4(s), 133.7(s), 131.6(s), 130.7(s), 130.2(s), 128.1(s), 126.9(s). δ_{Te} (81.2 MHz, CDCl_3): 848.0. m/z (ES^+): 490.68 ($[\text{M} - \text{I}_2 + \text{OMe}]^+$, 100%).

Compound **15**. A solution of (8-phenylsulfanyl)naphth-1-yl)diphenylphosphine, **D8** (0.30 g, 0.71 mmol), in dichloromethane (15 mL) was treated with bromine (0.45 g, 0.15 mL, 2.8 mmol). An analytically pure sample was obtained by crystallization from the diffusion of dichloromethane into a pentane solution of the product (0.2 g, 32%). ν_{\max} (KBr disk)/ cm^{-1} : 3430brs, 3069w, 3052w, 2691w, 2197w, 1968w, 1898w, 1814w, 1738w, 1636w, 1578s, 1543w, 1477vs, 1435vs, 1320s, 1264w, 1197s, 1151s, 1115vs, 1064w, 1023w, 988w, 921w, 887s, 825s, 765vs, 738vs, 718vs, 687vs, 625w, 613w, 581w, 561vs, 535vs, 503s, 468s, 413s, 346vs. δ_{H} (270 MHz, CDCl_3): 8.41 (1 H, d, *J* 8.0 Hz, nap 4-H), 8.25 (1 H, d, *J* 8.0 Hz, nap 5-H), 7.87 (2 H, d, *J* 6.8 Hz, nap 2,7-H), 7.69 (1 H, t, *J* 7.7 Hz, nap 6-H), 7.66–7.59 (1 H, m, nap 3-H), 7.57–7.42 (6 H, m, 2 × *PPH_2* 3–5-H), 7.41–7.30 (4 H, m, 2 × *PPH_2* 2,6-H), 6.96 (1 H, t, *J* 7.3 Hz, *SPh* 4-H), 6.92–6.83 (2 H, m, *SPh* 3,5-H), 6.15 (2 H, d, *J* 7.5 Hz, *SPh* 2,6-H), 2.99 (1 H, br s, –OH). δ_{C} (67.9 MHz, CDCl_3): 140.6(s), 137.3(s), 132.8(s),

132.6(s), 131.5(d, *J* 10.4 Hz), 129.2(d, *J* 13.5 Hz), 128.7(s), 128.2(s), 128.1(s), 126.2(s), 125.7(s), 125.5(s). δ_{P} (109 MHz, CDCl_3): 52.48. m/z (ES^+): 458.85 ($[\text{M} - \text{Br}_3 + \text{Na}]^+$, 100%).

5.1. Crystal Structure Analyses. X-ray crystal structures determined for compounds **8** and **10** were collected at $-180(1)^\circ\text{C}$ by using a Rigaku MM007 high brilliance RA generator (Mo $K\alpha$ radiation, confocal optic) and Mercury CCD system. At least a full hemisphere of data was collected using ω scans. Intensities were corrected for Lorentz, polarization and absorption. Data for all other compounds [**1–5**, **7**, **9–15**] were collected at $-148(1)^\circ\text{C}$ on the St. Andrews STANDARD system⁷⁷ Rigaku ACTOR-SM, Saturn 724 CCD area detector with confocal optic Mo $K\alpha$ radiation ($\lambda = 0.71073 \text{ \AA}$). The data were corrected for Lorentz, polarization, and absorption. The data for the complexes analyzed were collected and processed using CrystalClear (Rigaku).⁷⁸ The structure was solved by direct methods⁷⁹ and expanded using Fourier techniques.⁸⁰ The non-hydrogen atoms were refined anisotropically. Hydrogen atoms were refined using the riding model. All calculations were performed using the CrystalStructure⁸¹ crystallographic software package except for refinement, which was performed using SHELXL-97.⁸²

5.2. Computational Details. Geometries were fully optimized in the gas phase at the B3LYP level⁸³ using Curtis and Binning's 962(d) basis⁸⁴ on Se and Br (augmented with a set of diffuse s and p functions on Br) and 6-31+G(d) basis elsewhere, followed by calculation of the harmonic frequencies to confirm the minimum character of each stationary point and to evaluate standard thermodynamic corrections at 1 atm and 298 K. Wiberg bond indices⁷⁶ were obtained in a natural bond orbital⁸⁵

(77) Fuller, A. L.; Scott-Hayward, L. A. S.; Li, Y.; Bühl, M.; Slawin, A. M. Z.; Woollins, J. D. *J. Am. Chem. Soc.* **2010**, *132*(16), 5799.

(78) *CrystalClear 1.6*; Rigaku Corporation: Tokyo, 1999. *CrystalClear Software User's Guide*, Molecular Structure Corporation: The Woodlands, TX, 2000. Flugrath, J. W. P. *Acta Crystallogr., Sect. D: Biol. Crystallogr.* **1999**, *D55*, 1718.

(79) SIR97: Altomare, A.; Burla, M.; Camalli, M.; Casciarano, G.; Giacovazzo, C.; Guagliardi, A.; Moliterni, A.; Polidori, G.; Spagna, R. *J. Appl. Crystallogr.* **1999**, *32*, 115.

(80) DIRDIF99: Beurskens, P. T.; Admiraal, G.; Beurskens, G.; Bosman, W. P.; de Gelder, R.; Israel, R.; Smits, J. M. M. The DIRDIF-99 program system, Technical Report of the Crystallography Laboratory, University of Nijmegen, The Netherlands, 1999.

(81) *CrystalStructure 3.8.1: Crystal Structure Analysis Package*, Rigaku and Rigaku/MS: The Woodlands, TX, 2000–2006.

(82) SHELX97: Sheldrick, G. M. *Acta Crystallogr., Sect. A: Found. Crystallogr.* **2008**, *64*, 112.

(83) (a) Becke, A. D. *J. Chem. Phys.* **1993**, *98*, 5648. (b) Lee, C.; Yang, W.; Parr, R. G. *Phys. Rev. B* **1988**, *37*, 785.

(84) Binning, R. C.; Curtiss, L. A. *J. Comput. Chem.* **1990**, *11*, 1206.

(85) Reed, A. E.; Curtiss, L. A.; Weinhold, F. *Chem. Rev.* **1988**, *88*, 899.

(86) As implemented in G03: (a) Barone, V.; Cossi, M.; Tomasi, J. *J. Comput. Chem.* **1998**, *19*, 404–417. (b) Cossi, M.; Scalmani, G.; Rega, N.; Barone, V. *J. Chem. Phys.* **2002**, *117*, 43–54. (c) Cossi, M.; Crescenzi, O. *J. Chem. Phys.* **2003**, *119*, 8863–8872.

(87) Boys, S. F.; Bernardi, F. *Mol. Phys.* **1970**, *19*, 553.

(88) Frisch, M. J.; Trucks, G. W.; Schlegel, H. B.; Scuseria, G. E.; Robb, M. A.; Cheeseman, J. R.; Montgomery, J. A., Jr.; Vreven, T.; Kudin, K. N.; Burant, J. C.; Millam, J. M.; Iyengar, S. S.; Tomasi, J.; Barone, V.; Mennucci, B.; Cossi, M.; Scalmani, G.; Rega, N.; Petersson, G. A.; Nakatsuji, H.; Hada, M.; Ehara, M.; Toyota, K.; Fukuda, R.; Hasegawa, J.; Ishida, M.; Nakajima, T.; Honda, Y.; Kitao, O.; Nakai, H.; Klene, M.; Li, X.; Knox, J. E.; Hratchian, H. P.; Cross, J. B.; Bakken, V.; Adamo, C.; Jaramillo, J.; Gomperts, R.; Stratmann, R. E.; Yazyev, O.; Austin, A. J.; Cammi, R.; Pomelli, C.; Ochterski, J. W.; Ayala, P. Y.; Morokuma, K.; Voth, G. A.; Salvador, P.; Dannenberg, J. J.; Zakrzewski, V. G.; Dapprich, S.; Daniels, A. D.; Strain, M. C.; Farkas, O.; Malick, D. K.; Rabuck, A. D.; Raghavachari, K.; Foresman, J. B.; Ortiz, J. V.; Cui, Q.; Baboul, A. G.; Clifford, S.; Cioslowski, J.; Stefanov, B. B.; Liu, G.; Liashenko, A.; Piskorz, P.; Komaromi, I.; Martin, R. L.; Fox, D. J.; Keith, T.; M. A. Al-Laham, Peng, C. Y.; Nanayakkara, A.; Challacombe, M.; Gill, P. M. W.; Johnson, B.; Chen, W.; Wong, M. W.; Gonzalez, C.; Pople, J. A. *Gaussian 03*, Revision E.01; Gaussian, Inc.: Wallingford, CT, 2004.

analysis at the same level. The optimizations were started from the experimental structures available from X-ray crystallography, substituting chalcogens and halogens where necessary. Additional single-point energy calculations were performed using the polarizable continuum model (PCM) of Tomasi and co-workers,⁸⁶ employing the same basis sets on Se and Br as before, and 6-311+G(d) elsewhere, together with the parameters of CH₂Cl₂ as a typical solvent. The resulting changes in relative energies were added as increments to the gas-phase free energies, affording the $\Delta G_r(\text{CH}_2\text{Cl}_2)$ values in Figure 13. Reaction energies have not been corrected for basis-set superposition error (BSSE). An exploratory BSSE calculation for **C** using the Counterpoise method⁸⁷ (with **D2** and Br₂ fragments) indicated a very small correction of just around 1 kcal/mol. The com-

putations were performed using the Gaussian 03 suite of programs.⁸⁸

Acknowledgment. Elemental analyses were performed by Sylvia Williamson, and Mass Spectrometry was performed by Caroline Horsburgh. Calculations were performed using the EaStCHEM Research Computing Facility maintained by Dr. H. Früchtl. The work in this project was supported by the Engineering and Physical Sciences Research Council (EPSRC). M.B. thanks EaStCHEM for support.

Supporting Information Available: Crystal structure illustrations for compounds **3**, **5**, **8–10**, and **12–14** and CIF data for **1–15**. This material is available free of charge via the Internet at <http://pubs.acs.org>.